VERIFICATION AND COMPARISON OF POLAR MM5 AND AFWA MM5 FORECASTS OVER ALASKA

THESIS

William E. Courtemanche, Captain, USAF

AFIT/GM/ENP/02M-02

DEPARTMENT OF THE AIR FORCE
AIR UNIVERSITY

AIR FORCE INSTITUTE OF TECHNOLOGY

Wright-Patterson Air Force Base, Ohio

APPROVED FOR PUBLIC RELEASE; DISTRIBUTION UNLIMITED.

Report Documentation Page

Report Date	**Report Type**	**Dates Covered (from... to)**
26 Mar 02	Final	Jun 01 - Mar 02

Title and Subtitle verification and Comparison of Polar MM5 and AFWA MM5 Forecasts over Alaska	**Contract Number**
	Grant Number
	Program Element Number
Author(s) Captain William E. Courtemanche, USAF	**Project Number**
	Task Number
	Work Unit Number
Performing Organization Name(s) and Address(es) Air Force Institute of Technology Graduate School of Engineering and Management (AFIT/EN) 2950 P Street, Bldg 640 WPAFB OH 45433-7765	**Performing Organization Report Number** AFIT/GM/ENP/02M-02
Sponsoring/Monitoring Agency Name(s) and Address(es) Dr. Jerry Wegiel AFWA/DNXM 106 Peacekeeper Dr. Offutt AFB, NE 68113-4039	**Sponsor/Monitor's Acronym(s)**
	Sponsor/Monitor's Report Number(s)
Distribution/Availability Statement Approved for public release, distribution unlimited	
Supplementary Notes The original document contains color images.	

Abstract
The Mesoscale Model 5th Generation (MM5) is used for operational support to Air Force missions in the Alaskan Theater. The 11th Operational Weather squadron has identified problems with the MM5 producing excessively warm surface temperatures. The Polar MM5 (PMM5), developed by the Byrd Polar Research Center for high latitude ice sheets, is tested over the Alaskan domains used by the Air Force Weather Agency to determine the utility in replacing the MM5 with the PMM5. The verification of surface temperature, pressure and wind as well as upper-air temperature, geopotential height, and relative humidity of 27-hour PMM5 forecasts are compared to the MM5 forecasts to assess the differences between the models' accuracies. A grid-to-station technique is used to compare model output to surface observation for 68 locations and to radiosonde upper-air observations for 7 locations. The MM5 outperformed the PMM5 in root mean square error of all surface and upper-air parameters, while the PMM5 exhibited smaller biases in all fields. The differences between the models fell within the measurement accuracies of all parameters expect temperature. The analysis of horizontal features and comparison of domain biases alludes to a more physically realistic solution of the PMM5. The bottom line of site forecast accuracy precludes replacing the MM5 with the PMM5 at this time.

Subject Terms
Mesoscale Model, Polar Mesoscale Modeling, MM5, PMM5, Air Force Weather Agency, AFWA MM5, Numerical Weather Prediction, Model Comparison, Alaska Mesoscale Model, Alaska Temperature Forecast, Alaska Radiation, High-Latitude Radiation, High-Latitude Moisture, Atmospheric Temperature, Weather

Report Classification	**Classification of this page**
unclassified	unclassified
Classification of Abstract	**Limitation of Abstract**
unclassified	UU

Number of Pages
94

The views expressed in this thesis are those of the author and do not reflect the official policy or position of the United States Air Force, Department of Defense or the U.S. Government.

AFIT/GM/ENP/02M-02

VERIFICATION AND COMPARISON OF POLAR MM5 AND AFWA MM5 FORECASTS OVER ALASKA

THESIS

Presented to the Faculty

Department of Engineering Physics

Graduate School of Engineering and Management

Air Force Institute of Technology

Air University

Air Education and Training Command

In Partial Fulfillment of the Requirements for the

Degree of Master of Science in Meteorology

William E. Courtemanche, B.S.

Captain, USAF

March 2002

APPROVED FOR PUBLIC RELEASE; DISTRIBUTION UNLIMITED

AFIT/GM/ENP/02M-02

VERIFICATION AND COMPARISON OF POLAR MM5 AND AFWA MM5 FORECASTS OVER ALASKA

William E. Courtemanche, B.S.

Captain, USAF

Approved:

Michael K.Walters Advisory Committee Chairman	6 MAR 02 Date
Devin J. Della-Rose Advisory Committee Member	6 Mar 02 Date
Edward D. White Advisory Committee Member	8 Mar 02 Date

Acknowledgements

Conducting research in the interdisciplinary field of Numerical Weather Prediction requires a very large toolbox of knowledge that could not be found at the local Sears or Home Depot; I looked. I required assistance from many individuals to help me fill this very empty toolbox. I need to thank Lt Col Mike Walters, my thesis advisor, for helping get my feet off the ground as we muddled through the initial computer hurdles together. I am also (grudgingly) grateful for his torturous tests of computational assurance by branding the question "How do you know it's right?" into the back of my head. This led me to the brink of insanity by performing calculations in several manners to ensure that my results were accurate, building redundancy into my programs, and bringing me to the point of exchanging a 586-processor supercomputer for a mechanical pencil and paper. Honestly, thank you sir.

I received considerable help from Dr. Jim Bresch at the National Center for Atmospheric Research, Dr. Jeff Tilley at the University of Alaska Fairbanks, and Dr. Dave Bromwich at the Byrd Polar Research Center in getting the PMM5 compiled and running. This project would not have been possible without the dedication of the DOC4 team at the Air Force Combat Climatology Center, especially SSgt Scott Houston and MSgt Stephen Foster. Finally, I would like to thank my peers for the persistent jocularity that kept us all sane and for the few valuable nuggets of professional interaction and scrutiny, especially from Captains Patricia Vollmer and Dean Carter, and 1Lt Rob Evans. I would like to thank my family for their support in understanding my temporary absence while working on this project.

William E. Courtemanche

Table of Contents

List of Figures

Page

List of Tables

Page

List of Acronyms

3DVAR	3-Dimensional Variational Analysis System
AFB	Air Force Base
AFIT	Air Force Institute of Technology
AFS	Air Force Station
AFWA	Air Force Weather Agency
agl	Above Ground Level
AMPS	Antarctic Mesoscale Prediction System
AST	Alaska Standard Time
AVN	Aviation Model
BPRC	Byrd Polar Research Center
CCM2	Community Climate Model, version 2
CLW	Cloud Liquid Water
CONUS	Continental United States
DoD	Department of Defense
ENP	Engineering Physics Department
FDDA	4-Dimensional Data Assimilation
GM	General Meteorology Program
gpm	Geopotential Meter
K	Degrees Kelvin
MDAS	Mesoscale Data Assimilation System
MM5	Mesoscale Model 5th Generation
MPI	Multiprocessor Instruction
MSL	Mean Sea Level
MSRC	Major Shared Resource Center
MVOI	Multivariate Optimum Interpolation
NCAR	National Center for Atmospheric Research
NCEP	National Center for Environmental Prediction
NSIDC	National Snow and Ice Data Center
NWP	Numerical Weather Prediction
OMP	Open Multiprocessor
OWS	Operational Weather Squadron
PBL	Planetary Boundary Layer
PMM5	Polar Mesoscale Model 5th Generation
PSU	Pennsylvania State University
RAOB	Radiosonde Observation
RH	Relative Humidity
RIP	Read/Interpolate/Plot
RMSE	Root Mean Square Error
RMSVE	Root Mean Square Vector Error
SiB	Simple Biosphere
UCAR	University Corporation for Atmospheric Research
USAF	United States Air Force
USGS	United States Geological Survey
UTC	Universal Time Code

Abstract

The Mesoscale Model 5th Generation (MM5) is used for operational support to Air Force missions in the Alaskan Theater. The 11th Operational Weather squadron has identified problems with the MM5 producing excessively warm surface temperature forecasts. The Polar MM5 (PMM5), developed by the Byrd Polar Research Center for the high latitude ice sheets of Antarctica and Greenland, is tested over the Alaskan domains used by the Air Force Weather Agency to determine the utility in replacing the MM5 with the PMM5. The verification of surface temperature, pressure and wind as well as upper-air temperature, geopotential height, and relative humidity of 27-hour PMM5 forecasts are compared to the MM5 forecasts to assess the differences between the models' accuracies. A grid-to-station inverse-weighted linear interpolation technique is used to compare model output to surface observation for 71 locations and to radiosonde upper-air observations for 7 locations. The results are based on 67 forecasts made over a 4-month period during the Fall-Winter of 2001.

The MM5 outperformed the PMM5 in root mean square error of all surface and upper-air parameters, while the PMM5 exhibited smaller biases in all fields. The differences between the models fell within the measurement accuracies of all parameters expect temperature. The lack of assimilated snow cover may be responsible for the warm bias of both models in the winter months. The analysis of horizontal features and comparison of domain biases alludes to a more physically realistic solution of the PMM5. The bottom line of site forecast accuracy precludes replacing the MM5 with the PMM5 at this time.

VERIFICATION AND COMPARISON OF POLAR MM5 AND AFWA MM5 FORECASTS OVER ALASKA

I. Introduction

1.1. Air Force Relevance

The dependence on meteorological forecast models to produce a weather forecast is continually increasing. This dependence can be cited for a number of reasons such as increased operational tempo, improved computing power, smarter software, and debatably the most important factor, decreased forecaster experience. The current Air Force weather forecaster experience level has decreased recently for a variety of operations tempo and manning issues. This experience deficiency results in a strong reliance on meteorological models. This thesis will hopefully provide an improvement to the accuracy of this important tool at the disposal of the Air Force weather forecaster.

The 11th Operational Weather Squadron (OWS) at Elmendorf AFB, AK has proposed this topic to enhance their support to operations over the Alaskan theater. The enormous domain and high latitude of the Alaskan theater lends itself to meteorological extremes. Alaska experiences extreme meteorological phenomena exceeding that of the mid-latitude region, particularly in temperature statistics. The 11th OWS provides the meteorological support for the Alaskan theater of operations. Department of Defense (DoD) assets include 2 major Air Force installations, Elmendorf and Eielson Air Force Bases (AFB); 3 major Army

installations, Forts Richardson and Wainwright, and Allen Army Airfield; a remote radar site, Clear Air Force Station; and several remote communication, radar, and reserve airfields locations. The Alaskan theater is the operating region for these residing units, but also serves as a unique and popular training region for many CONUS based units as well as numerous annual international training venues. Support from the 11th OWS is crucial to the safety of all DoD assets in such a harsh and desolate environment.

The Fifth-Generation Pennsylvania State University (PSU)/National Center for Atmospheric Research (NCAR) Mesoscale Model (MM5) was developed for the mid-latitudes. The MM5 produces a weather forecast using a variety of user-specified sets of physics equations. The specialized sets of equations, or parameterization schemes, were developed for various specialized applications, none of which were designed for the Polar Region. There has been limited modification to tailor the model for a high-latitude application. One of the most prominent discrepancies noted by the 11th OWS in the model output is the surface temperature. The greatest errors occur in extreme conditions, such as during a strong Arctic radiation inversion when surface temperatures persist below –40ºC for several days.

1.2. Problem Statement

The application of mid-latitude physics parameterizations in the MM5 over Alaska generates persistent errors in output, specifically in the surface temperature field. Excessive longwave radiation from high ice cloud concentrations has been identified as the major contributor to this error (Bromwich, 2001a; Tilley, 2001; and Manning and Davis, 1997). Modifications have been made to the MM5 to help mitigate these errors. The Byrd Polar

Research Center (BPRC), The Ohio State University, made the modifications specifically for the polar ice sheets of Greenland and Antarctica. A verification of this modified Polar MM5 (PMM5) over Alaska is necessary to determine the applicability of the modifications to the Alaskan theater. Finally, a comparison of the PMM5 to the operational MM5 used currently by the Air Force Weather Agency (AFWA) is needed to assess any differences.

1.3. Research Objectives

This research project will result in a recommendation to AFWA on the utility of the PMM5 for the Alaskan theater of operations. There were several research objectives necessary to arrive at a sound assessment of an Alaskan application of the PMM5.

1. Compile and run the MM5
2. Compile and run the PMM5
3. Develop and execute a verification procedure
4. Compare the verification results differences between the MM5 and AFWA MM5
5. Compare the verification results differences between the MM5 and PMM5
6. Determine the significance of the differences between the MM5 and PMM5

Each of the objectives was approached with the principle of mirroring the AFWA production MM5. Great care was given in maintaining this principle to ensure that these results would most accurately reflect results that could be obtained by running the PMM5 operationally at AFWA. The verification objectives were designed to duplicate the verification process used by AFWA to ensure consistent statistical results. AFWA's verification results were available to make an assessment of this consistency.

The first objective required modification to the model programming code in order to run the model with the exact input used in the AFWA operational MM5. The appropriate FORTRAN compilers were only recently acquired by AFIT to make this project feasible with our existing computing architecture. This project was one of the first independent study projects at AFIT implementing the MM5, and this generated numerous computing obstacles. The Aeronautical System Center Major Shared Resource Center (MSRC) IBM SP P3 was used to make the actual model runs. Learning to use and obtaining access to the MSRC provided a substantial obstacle in achieving the first two objectives.

1.4. Research Focus

This project was aimed at determining the forecast accuracy of the PMM5 over the Alaskan theater. This required some source code modification for use by AFWA, but did not extend to the level of modifying the model physics. The measurement of accuracy, or verification, was directed at duplicating AFWA seasonal verification products. This consisted of measuring the degree of model error compared to surface observations and radiosonde observations (RAOB). The hypothesized sources of model error, most pronounced in the temperature field, are the ice cloud-radiation interaction and planetary boundary layer (PBL), interactions (Bromwich et al. 2001b; Tilley 2001; Manning and Davis, 1997). This hypothesis provided the focus on moisture, radiation, and PBL physics of the MM5 for this project.

1.5. Assumptions/Limitations

The main limitation to this project was both real and processor time. The number of model runs was maximized given the finite time and computing hours available, and the input data limitation of a 30-day archive. This project compares PMM5 forecasts (experiment) to MM5 forecasts (control) assumed to be equivalent to AFWA MM5 forecasts. Initialization limitations of the PMM5 necessitated making separate MM5 runs to make a statistically relevant comparison. Specifically, the type of model initialization used by AFWA is not possible with the PMM5. It was necessary to employ the same initialization process between the experimental (PMM5) and control (MM5) forecasts.

1.6. Summary of Results

The findings of this research do not present sufficient support for replacing the AFWA MM5 with the PMM5 for operational use. The MM5 was found to generate a warm bias in Alaska to substantiate the conjecture of the operational forecaster. The PMM5 corrected this bias in temperature as well as a pressure bias, however the overall skill measured by root mean square error of the PMM5 was inferior to the MM5. Both models exhibited similar responses for most upper-air quantities verified. An exception to these similarities was found in low-level moisture bias where the PMM5 produced a greater moist bias over the MM5 below 800 mb.

II. Background

2.1. General Polar Meteorology

This project was focused on forecasting for Alaska. Alaska is defined as an Arctic Region for the purposes of this work. Figure 1 identifies the specific region of interest. Some of the most significant meteorological differences between polar and mid-latitude regions derive from the difference in solar radiation. Other factors enhancing the latitudinal differences include temperature, surface albedo, airmass advection, and local distribution of land and water. The Arctic Ocean has a warming effect on the entire arctic region. Cracks (leads) and open areas in the sea ice (polynyas) permit intense heat exchange from the water

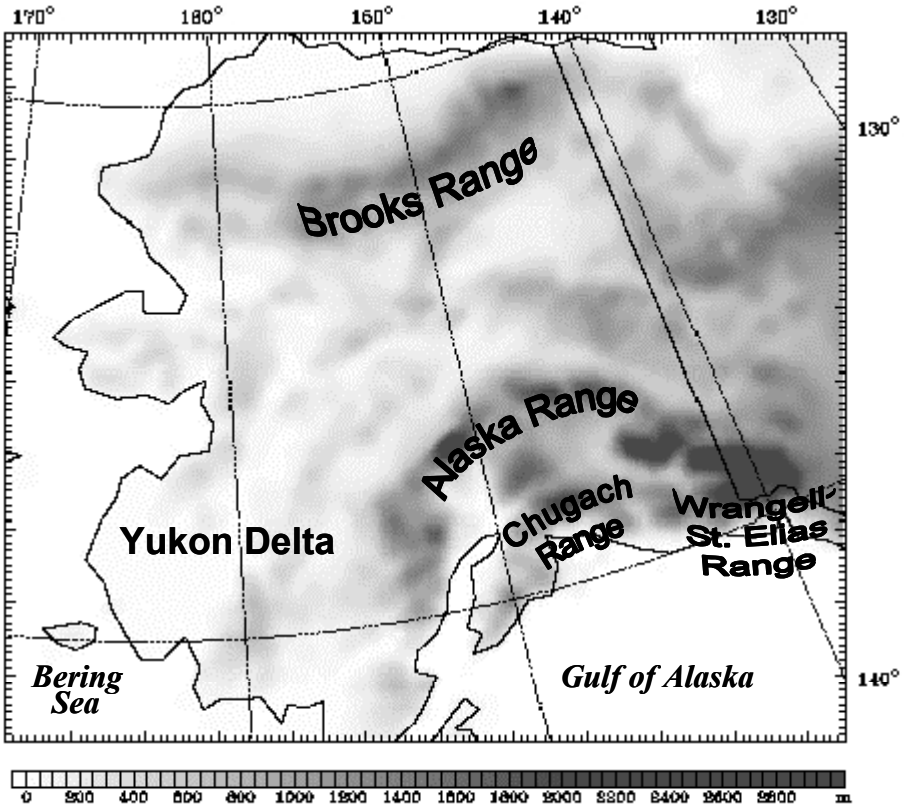

Figure 1. Map of Alaskan Domain of Interest. Relief map of Alaska annotated with the major mountain ranges that separate the major climatic regions of the area.

to the atmosphere during the winter (National Snow and Ice Data Center (NSIDC), 2001). This results in a warmer climate when compared to the Antarctic region. Section 2.4 covers these factors affecting temperature in great depth.

Continental regions exhibit larger seasonal variations in climate due to the lower heat capacity of the surrounding land compared to that of water surrounding a maritime region. Most of the region of interest is over land. The Alaskan region separates the Pacific Ocean from the Arctic Ocean, providing a significant climatic gradient across the area. The semi-permanent Aleutian Low spawns many of the synoptic cyclones that affect Alaska.
The Alaskan terrain isolates the region into several climatic zones. The Brooks Range restricts much of the Arctic Ocean influence to the North Slope, likewise the Alaska Range restricts much of the Pacific Ocean influence to the southern regions. The Interior falls between these two major mountain ranges and experiences a continental climate. The Interior experiences the greatest seasonal changes and some of the most extreme weather phenomena in North America.

2.2. General Numerical Weather Prediction

The advent of computers and their perpetual advancement has made numerical weather prediction (NWP) one of the most valuable tools in preparing operational forecasts. The numerical weather model consists of three parts; data analysis, dynamical computations, and physics computations. Data analysis is the process of assimilating measured observations to slightly modify a previous forecast. The modified forecast is used as a first guess from which the new forecast is based. There are numerous methods of data assimilation, which can produce very different initial conditions for a forecast.

Dynamical computations involve solving the equations that govern the forcing of air by mechanisms such as advection, heating and cooling, or pressure gradient. The sets of dynamic equations are comprised of vertical and horizontal momentum, thermodynamic, mass conservation equations. The physical computations encompass the parameterizations, interactions with exterior fluxes of energy, water, and momentum through the domain boundary, and cloud and precipitation processes. Modifications of the physical computations are the focus of this project.

2.3. Alaska Temperature Forecasting

Forecasting the weather requires an assessment of the fluxes of atmospheric energy and mass. Energy is determined by the magnitude of physical fluxes and can be related to wind speed whereas, mass can be related to moisture content and temperature. A temperature forecast generally results from the culmination of forecasting other atmospheric phenomena. Air-mass identification is a prerequisite in preparing an accurate temperature forecast. The composition of an airmass determines its thermodynamic response to physical processes such as evaporation, condensation, and radiation. The composition of the Earth's surface has a strong influence on the near-surface atmosphere. The land surface type affects parameters such as temperature and determines the turbulent energy distribution in the planetary boundary layer.

Land surface types such as sea ice, permafrost, and permanent glacial ice fields are significant factors not accounted for in mid-latitude forecasting. These surface types have very different thermal properties that are not accounted for in the MM5. The exclusion of these land surface types may be a contributing factor to the established warm tendency of the

MM5 over Alaska. The higher albedos of snow and ice surfaces reduce the thermal energy available to warm the atmosphere when compared to bare ground.

Regions of permafrost have highly saturated surfaces resulting from the lack of drainage due to the underlying frozen substrate. This can create a pitted landscape covered with pools of standing water, such as the North Slope of Alaska (region north of the Brooks Range). The excess soil moisture in these regions impacts the local radiation budget due to the high thermal capacity of water compared to dry ground.

The ability to accurately forecast the temperature requires an assessment of the local atmosphere radiation balance. The global solar radiation deficit in the Polar Regions and surplus in the equatorial regions results in colder temperatures in the Arctic and Antarctic Regions. The high solar zenith angle provides a low concentration of incoming solar radiation (insolation) at the Earth's surface compared to lower-latitude regions. This results in a surface temperature inversion persisting over much of Alaska for most of the winter. Summer temperature forecasting in Alaska is similar to mid-latitude forecasting with differential heating producing air-mass thunderstorms and morning inversions that break during the day. Moisture content is also an important temperature-forecasting factor as it affects the efficiency of radiation transmission.

2.4. Polar Radiation Budget

2.4.1. General Radiation. The round shape of the Earth creates a differential in the intensity of solar radiation density received at the surface between the equator and the poles, which creates the aforementioned solar radiation deficit at the poles. The absorption and emission of the earth-atmosphere system define the radiation budget. H_2O and CO_2 are

major factors in maintaining this balance by absorbing sufficient long-wave emissions from the surface to retain significant amounts of thermal energy in the atmosphere; hence these are considered greenhouse gases. Figure 2 represents the Arctic's annual radiation energy balance. On bare land solar radiation is absorbed by soil and re-radiated as heat. The solar radiation energy absorbed by ice and snow is spent melting ice and snow, keeping the temperatures low. The annual net radiation flux out of the Arctic atmosphere roughly balances the net advection of heat energy northward into the region (NSIDC, 2001).

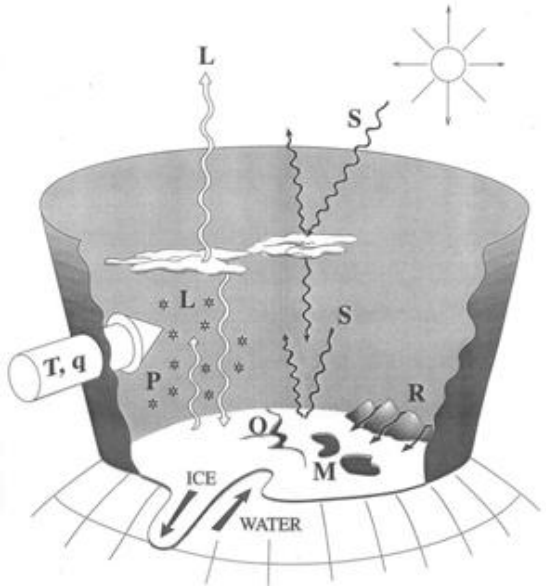

R = Runoff (freshwater)
L = Longwave radiation
S = Shortwave radiation
O = Ocean heat
M = Melt (snow and ice)
P = Precipitation
T = Temperature (heat transfer)
q = moisture

Figure 2. Arctic Region Annual Radiation Energy Balance. Schematic of radiation fluxes in the earth-atmosphere system. Adapted from NSIDC Arctic Climatology and Meteorology Primer (2001).

2.4.2. Effects of High-Level Clouds. Clouds heavily influence the radiation budget and therefore temperature by reflecting a large fraction of solar radiation, which results in surface cooling. Alternatively, clouds inhibit long-wave radiation loss from the surface, which can lead to higher surface temperatures. The dominant process depends on many factors including cloud type and thickness, the magnitude of the solar radiation, and the albedo of the underlying surface. The radiative effect of high-level clouds varies significantly from that of middle and low clouds due to differences in composition. The shallow, cold

environment of the Polar Regions results in more ice clouds, ranging from scattered wisps of cirrus to dense cirrostratus layers, when compared to the lower-latitude atmosphere. Ice crystals are accepted as hexagonal columnar shaped (Rogers and Yau, 1996) and have different reflective properties and phase functions from those of spheres, such as liquid water droplets of lower, warmer clouds.

Emissivity (ε) is an important radiative characteristic of a substance examined to assess its role in the radiation budget. Emissivity is defined as the ratio of radiant energy emitted (E) to absorptivity (a) at a specific wavelength (λ),

$$\varepsilon = \frac{E_\lambda}{a_\lambda}. \tag{1}$$

The emissivity of a substance is constant, for a specific λ, with a maximum value of unity. A blackbody is a substance with an emissivity of unity at all wavelengths. The emissivity of cirrus clouds range well below unity. It has been found that emissivity of cirrus clouds is a function of cloud thickness (Liou, 1974). Figure 3 shows the results from several studies. The dots, solid line, and dashed line represent three separate studies. These results show that

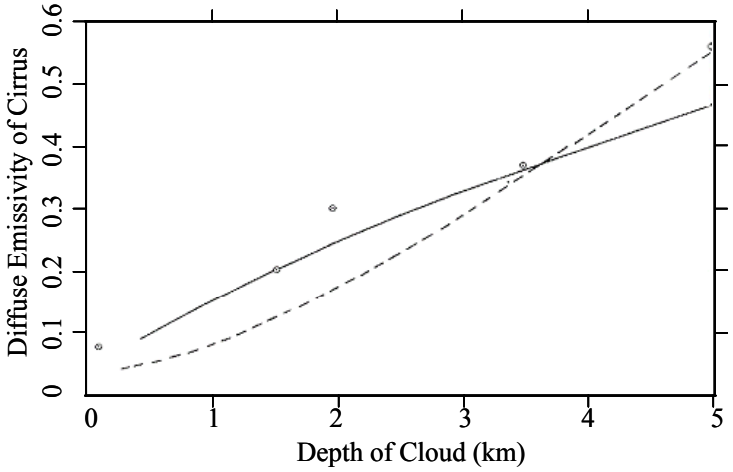

Figure 3. Cirrus Cloud Emissivity. These studies show the relationship of cirrus cloud emissivity to the depth of the cloud. Each trace/plot represents a different study. Adapted from Houghton (1985).

cirrus cloud depth is directly proportional to emissivity.

The presence of nocturnal cirrus clouds has the radiative effect of reflecting much of the longwave radiation of the earth back to the atmosphere and the surface. In their absence, this radiation is allowed to escape to space. The radiative significance of cirrus clouds is not only great in the Polar Regions at night, but also during the relatively high solar zenith angle periods of the day in the Alaskan winter. This is the basis for polar modifications to the moisture microphysics and radiation parameterization in the MM5.

2.5. General Description of MM5

2.5.1. MM5 Overview. The MM5 is a nonhydrostatic finite difference (centered in time and space) grid point model. A second order leapfrog scheme is used for the temporal differencing. For further description see Grell et al., 1995. The atmospheric motions represented by the model in this project are on a small enough scale to invalidate a hydrostatic approximation (Grell et al., 1995). The MM5 allows for a four-dimensional data-assimilation and uses numerous physical parameterizations schemes.

The MM5 modeling system consists of four pre-processors (TERRAIN, REGRID, RAWINS/little_r, and INTERP), the main model program (MM5), and a post-processor (GRAPH). An alternative post-processor Read/Interpolate/Plot (RIP) replaced the standard GRAPH program; both required the NCAR graphics software. Figure 4 depicts a schematic of the MM5 modeling system. The TERRAIN program assimilates a dataset from the 24-category Unites States Geographical Survey (USGS) data source, a PSU/NCAR Old 13 category data source, or a 16-category Simple Biosphere model (SiB) data source.

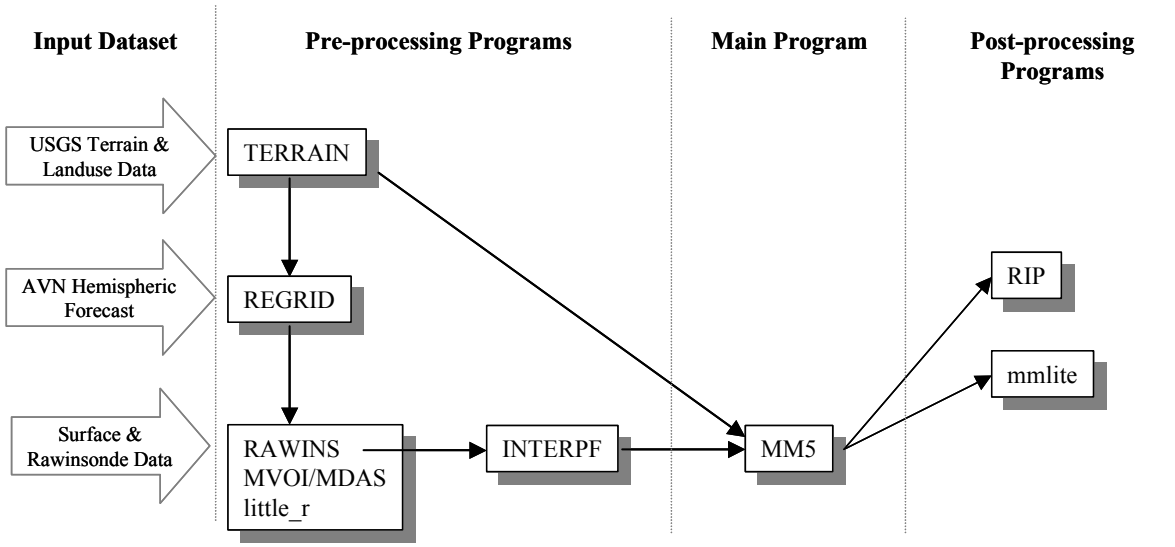

Figure 4. MM5 Modeling System. This flow chart shows the flow of data processing through the MM5 modeling system. There are three major subdivisions: pre-processing programs, main program processing, and post-processing routines.

TERRAIN defines the grid domain on the specified map projection. This research used 10 minute and 5 minute USGS data for the outer and inner domains respectively. Next, the TERRAIN coarse domain output along with the Aviation Model (AVN) forecast is passed into the REGRID program. The REGRID program reads in the meteorological analysis (first-guess), and interpolates the analysis to the model grid defined by the TERRAIN program. The output from REGRID is passed into an observation assimilation program RAWINS, Multivariate Optimum Interpolation (MVOI), or little_r to enhance the first-guess field using the input observations. AFWA currently uses MVOI to be replaced shortly by Three Dimensional Variational Analysis System (3DVAR). The final pre-processor, INTERPF, vertically interpolates the output from RAWINS and higher resolution TERRAIN to the vertical sigma coordinates of the model domain. INTERPF produces the initial and boundary conditions necessary to solve the meteorological equations in the MM5 main code. The main MM5 program requires the initial and boundary conditions generated by INTERPF as well as the TERRAIN output defining the domain.

One-way nesting interaction is used for all forecasts in this thesis work. Interaction describes the flow of data between the outer and inner domains. Two-way interaction involves feeding the outer domain with results from the inner nest, whereas one-way interaction only pushes data from the outer domain to the inner nest. Controversy exists over the ideal interaction method. One-way interaction has a tendency to dampen out errors that originate on the boundaries. Two-way interaction presents difficulties with small-scale features on the greater resolution nested domain, which may not be resolvable on the coarse outer domain (Vukicevic and Paegle, 1989).

The AFWA production MM5 uses one-way interaction. The model is run one nest at a time versus simultaneous nesting. A few test scenarios showed running the two separate domains with one-way interaction option ran approximately 20% faster than the nested two-way interaction option. Running the one-way interaction requires the additional program NESTDOWN found in the MM5 suite. Figure 5 illustrates the data flow through the NESTDOWN sequence. NESTDOWN creates the initial and boundary conditions for the inner domain using the MM5 output from the outer domain, the inner domain TERRAIN output, and the outer domain boundary output from INTERPF.

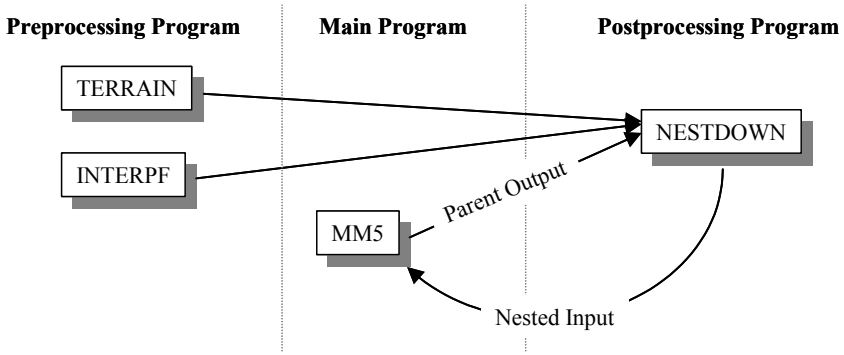

Figure 5. NESTDOWN Schematic. This diagram shows the NESTDOWN sequence for generating MM5 input files for the nested domain using one-way interaction.

2.5.2. Vertical Description. The selection of a vertical coordinate system is a significant determination in the ability of a model to accurately represent the atmosphere. Other models have used pressure levels and eta coordinate systems (fixed levels interrupted by terrain) however, the MM5 uses a sigma (σ) coordinate system, defined as a ratio of pressure differences:

$$\sigma = \frac{\left(p - p_t\right)}{\left(p_s - p_t\right)}, \tag{2}$$

where p_t is the specified constant top of the atmosphere pressure, p_s is the specified constant surface pressure, and p is a reference pressure at a given level. The reference pressure is a function of terrain height and user-defined constants: sea level pressure, sea level temperature, and lapse rate (Dudhia et al., 2001). Only terrain height varies over the domain, so the sigma levels remain at fixed heights above ground level throughout the forecast integrations. Sigma values range from zero at the defined top of the atmosphere to 1 at the surface. Figure 6 shows an example of a vertical cross section using 9 sigma levels. The lowest sigma level (σ=1.0) is terrain following and represents the bottom boundary of the model domain. The highest sigma level (σ=0.0) is the quasi-horizontal top of the atmosphere representing the top boundary of the model domain. The top layer (set to 50mb for this research) acts as a material surface that limits the flux of atmospheric properties across it and can be parameterized within the model physics. This flux of atmospheric properties across the top boundary, referred to as radiative, is critical in maintaining the energy balance in the

model. Grell et al. (1995) summarize the upper boundary condition developed by Klemp and Durran (1983) and Bougeault (1983) that allows wave energy to pass through unreflected.

INTERPF interpolates the MVOI output onto sigma levels. Parameters are set in INTERPF to define reference pressures at the top and bottom of the domain, and a reference temperature at sea level. The only variable is the surface elevation, which results in fixing each sigma level to a constant height above ground level (AGL) across the domain, referred to as 'terrain following'.

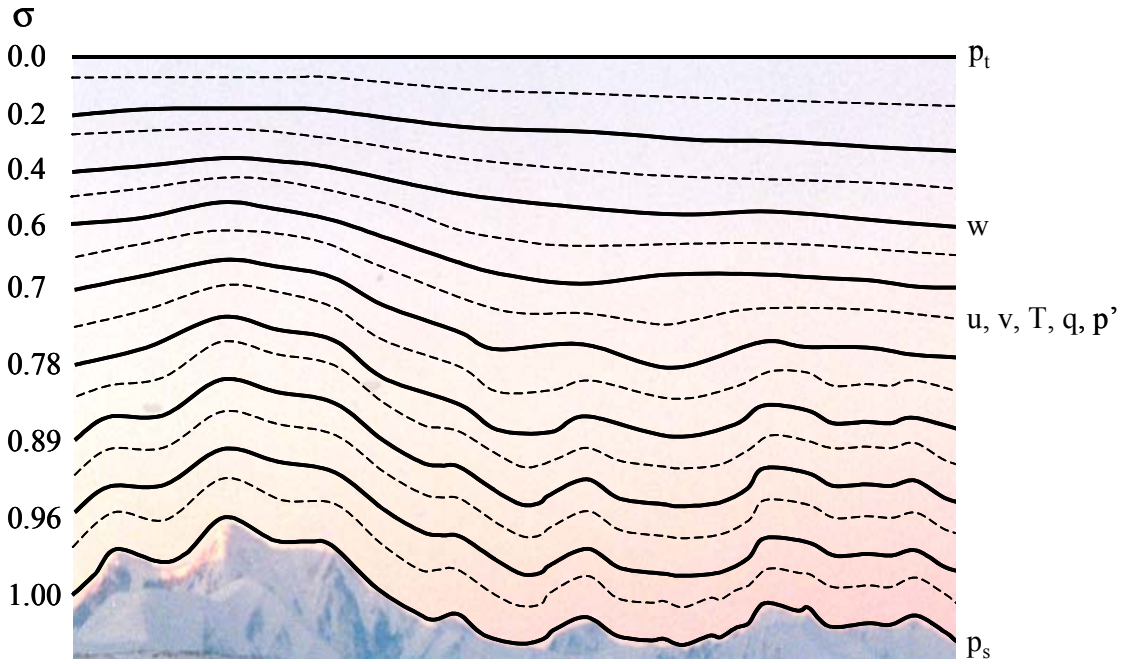

Figure 6. Sigma Coordinate System. Schematic representation of the vertical structure of the MM5. This example depicts a vertical resolution of 9 sigma levels. Dashed lines denote half-sigma levels and solid lines denote full-sigma levels. Vertical velocity is calculated on sigma levels, all other parameters are calculated on half-sigma levels.

The number of sigma levels (which do not have to be evenly spaced) defines the vertical resolution. The smaller scale motions in the planetary boundary layer dictate a higher density (resolution) of sigma levels than for the rest of the atmosphere above the PBL. Vertical velocity is defined at the full sigma level whereas all other variables are defined in the middle of each model vertical layer, referred to as half-sigma level.

2.5.3. Horizontal Description. MM5 uses the Arakawa-Lamb B staggering grid for horizontal finite difference calculations as shown in Figure 7. This 'B' grid co-locates east-west velocity components, north-south velocity components, and Coriolis force at the corners of the grid boxes, or dot points (•). In contrast the remaining variables are defined at the center of the grid boxes, or cross points (X). This staggering has (debatably) improved accuracy over other staggering schemes due to the location of the parameters for calculations such as divergence and vorticity in reference to the computed grid point (Arakawa and Lamb, 1977). The I and J directional unit vectors are opposite those found on a typical Cartesian Coordinate system to improve computational efficiency of array loops in FORTRAN.

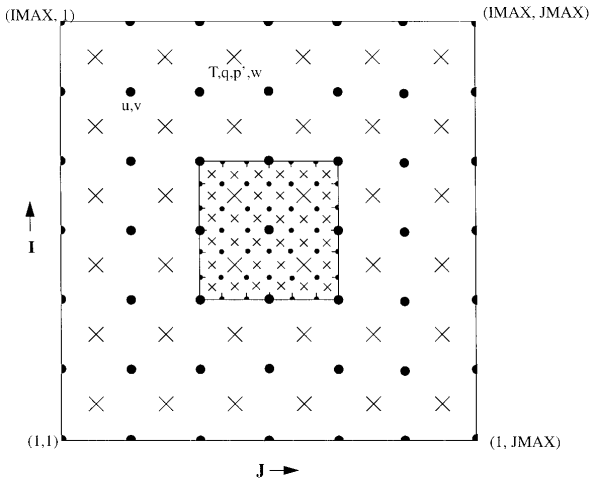

Figure 7. Arakawa-Lamb B Grid. This figure depicts a graphical representation of the staggered grid of parameters used by the MM5. Directional wind components and Coriolis force are defined at the dot points (•), while remaining variables are defined at the cross points (**X**). Adapted from Dudhia et al. (2001).

2.5.4. Parameterization. The model is not able to resolve atmospheric phenomena that occur on a scale smaller than the resolution of the model. Parameterization schemes are used to fractionalize processes that occur on scales smaller than the grid scale of the model domain. An example is cumulus parameterization, which is necessary unless the grid resolution is small enough (order of <5-10km) to encompass a cumulus cloud (Dudhia et al., 2001). The MM5 modeling system offers several options of parameterizations schemes for

cloud microphysics and precipitation processes, cumulus convection, radiative transfer, and PBL turbulence.

2.6. Description of Polar MM5 Modifications

The current version of MM5 (v3.4) allows for an abundance of options suitable for customizing forecasts of various types based in the mid latitudes. The model was not designed for a high latitude configuration or for a domain over an ice sheet such as Greenland or Antarctica. The BPRC has implemented several modifications to the MM5 such as adding a sea ice surface type, altering the parameterization of cloud radiation, replacing the standard ice concentration equation, and increasing soil substrate levels to account for environmental differences in high latitudes from the mid-latitude atmosphere. These modifications were designed specifically for Greenland and Antarctica. The performance of these modifications has not been quantified over a high-latitude, primarily non-ice covered landmass such as Alaska. Dr. Jeff Tilley is conducting similar research concurrently at the University of Alaska Fairbanks.

2.6.1. Explicit Moisture Modification. The PMM5 cloud and precipitation processes are represented by the Reisner 1 explicit microphysics parameterization (Reisner, 1998). This parameterization scheme predicts the mixing ratio of cloud water, rain water, snow water, and ice crystals and allows for the presence of mixed phase (partially frozen) clouds. Sub-grid scale clouds are parameterized with the unmodified Grell cumulus parameterization (Grell et al., 1995). Previous versions of the MM5 (MM4) were found to produce excessive cloud cover in the Polar Regions (Hines et al., 1997b) and (Manning and

Davis, 1997). Manning and Davis suggested a solution of replacing the equation for ice nuclei concentration (Fletcher, 1962),

$$n_c = 10^{-2} \frac{\exp[0.6(273.15 - T)]}{\rho} \tag{3}$$

with that of Meyers (1992),

$$n_c = 10^{3} \frac{\exp\left[-0.639 + 0.1296\left[100\left(S_i - 1\right)\right]\right]}{\rho} \tag{4}$$

in the Reisner 1 explicit moisture parameterization (n_c is ice-nuclei number concentration, r is air density, and S_i is the supersaturation with respect to ice). The cold temperatures found in the Polar Regions exceed the limits of validity of the Fletcher equation (Manning and Davis, 1997). This Fletcher equation replacement is proposed to help mitigate the cloudy bias in polar forecasts with the MM5.

The Reisner 1 mixed phase scheme computes cloud and rainwater fields explicitly with microphysical processes. Ice phase, supercooled water, and slow melting of snow are accounted for in the Reisner 1 scheme, however graupel and riming are not accounted for. Figure 8 represents the interactions between moisture phases accounted for in the Reisner 1

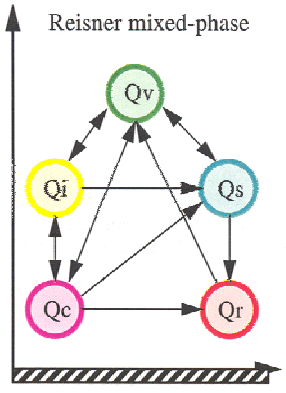

Figure 8. Reisner 1 Moisture Scheme. Graphical representation of the microphysics processes in the Reisner 1 mixed-phase explicit moisture parameterization. Q represents mixing ratio of the specific moisture phase: v-vapor, i-ice, c-cloud, s-snow, r-rain. Adapted from Dudhia et al. (2001).

explicit moisture parameterization. Cloud water is immediately frozen into cloud ice below –40°C, and cloud ice melts immediately at 0°C.

2.6.2. Radiation Modification. The PMM5 uses a modified version of the NCAR community climate model, version 2, (CCM2) radiation parameterization (Hack et al., 1993) to predict the radiative transfer of longwave and shortwave radiation through the atmosphere. Sensitivity simulations found that parameterizing cloud cover as a simple function of grid box relative humidity, with cloud liquid water path (CLW) determined from grid box temperature, resulted in a significant overestimate of CLW path. This excessive CLW produced large downwelling longwave radiation fluxes during the austral winter over Antarctica (Hines et al., 1997a, 1997b). This problem is resolved by using the modeled water and ice mixing ratios from the Reisner explicit moisture parameterization to determine the radiative properties of the predicted cloud cover. This modification provides consistency of radiative and microphysical properties of clouds while allowing for separate treatment of radiative properties of liquid and ice phase cloud particles. This principle is based on the CCM3 radiation parameterization following results from Ebert and Curry (1992).

2.6.3. Land-use Modification. The MM5 uses a user-modifiable table of physical parameters for each surface type defined at a grid point. Appendix A lists the physical parameters of surface types used in the PMM5. There are two sets of physical parameters used for summer (15 April to 15 October) and winter (15 October to15 April). The surface type grid is generated by TERRAIN. The parameters defined include albedo, moisture available, emissivity (at 9μm), roughness length, and thermal inertia. The original PMM5 modifications added a sea ice surface type to the Old 13-category data. This additional

category is either added to the model as an additional binary data file or calculated based on sea surface temperature and fraction based on climatological values. The sea ice surface type allows for fractional sea ice coverage in any oceanic grid point. Surface fluxes for sea ice grid points are calculated separately from open water and averaged before interacting with the overlying atmosphere (Bromwich et al., 2001b).

2.6.4. PBL Modification. The PMM5 uses the National Center for Environmental Prediction (NCEP) Eta model 1.5 order turbulence closure scheme to parameterize turbulent fluxes in the atmosphere and turbulent fluxes between the atmosphere and the surface. Modifications were necessary to account for the new sea ice surface type category. The thermal properties used in the soil model for snow and ice surface types are modified following Yen (1981). The number of substrate levels is increased from six to eight, increasing the resolved substrate depth from 0.47 m to 1.91 m. Table 1 lists the sea ice thickness categories (Bromwich et al., 2001b). Sea ice thickness varies from 0.23 m to 0.95 m and is dependent on the hemisphere and sea ice fraction at the grid point.

Table 1. PMM5 Sea Ice Thickness (from Bromwich et al., 2001b).

Northern Hemisphere	
concentration (% of grid box)	Thickness (m)
>0.9	0.95
0.6 - 0.9	0.47
<0.6	0.23
Southern Hemisphere	
All concentrations	0.23

III. Methodology

3.1. Overview

The main focus of this research was to quantify the differences in accuracy between the PMM5 and MM5 over Alaska. Five separate time periods are used in the forecasts; 15-18 September 2001, 1-7 October 2001, 25-31 October 2001, 14-21 November 2001, and 1-8 Dec 2001. These periods represent the climatic shift from fall into winter and contain several forecast regimes established by the 11th OWS. The current operational MM5 run by AFWA dictated the design of the experiment. The PMM5 was configured as similarly as possible to AFWA's operational MM5. The most significant unintentional difference between the control (MM5) and the experiment (PMM5) was in the model initialization. The AFWA production uses a four-dimensional data assimilation (FDDA) technique. It was not possible to use FDDA in this experiment because: a) the FDDA initialization option is not possible with the ETA PBL scheme; and b) the observation files ingested into the FDDA were not available.

3.2. Input Data

A finite difference model requires boundary conditions throughout the forecast length because of the finite domain. Previous forecasts from hemispheric or global models are often used to provide these prognostic conditions. AFWA assimilates the NCEP Aviation Model (AVN) forecast to generate the MM5 input data files. To ensure consistent data assimilation, PMM5 and MM5 forecasts used the same operational input files acquired from AFWA.

AFWA currently uses an MVOI scheme to process the MM5 input data from the AVN forecasts, surface observations, RAOB data, and ship reports.

3.3. Four Dimensional Data Assimilation (FDDA)

FDDA represents the dynamic link between objective analysis methods and the dynamic relationship of the prognostic equations used for either model initialization or for use of the model as an analysis/research tool. The alternative model initialization is to simply begin integration from the initial time without any assimilation, referred to as cold-starting. There are two major types of FDDA used in the MM5. The analysis method is an intermittent process of initialization using a subsequent forecast as a first guess. The station method is a dynamic initialization where forcing functions are added to the model equations to "nudge" the model state toward the observations. The nudging is performed using a Newtonian-relaxation technique.

Newtonian relaxation terms are added to the prognostic equations for temperature, wind, and water vapor. These terms relax the model towards observations, which are chronologically listed for a defined time period. AFWA uses the analysis method only for temperature and wind for three hours. The moisture nudging was specifically excluded to allow the model to spin-up more rapidly (Swanson, 2001).

AFWA uses the first method of FDDA for a three-hour period, for the previous set of observations before the initial forecast valid time, then begins the forward prediction three hours prior to the actual model run time to match the analysis. So a 00 UTC run begins with 21 UTC observations. FDDA is not used for the nested domain. The forecast begins six hours after the initial time of the parent domain to save computer-processing time.

3.4. Model Configuration

This section describes the configurations of the forecasts used in this project. The MM5 provides a host of options to alter the domain, resolution, constants, equation sets, parameterization schemes, etc. In every situation possible the exact configurations were duplicated after the AFWA production MM5. Table 2 shows the difference in configurations between the three MM5 versions. The only difference between the MM5 runs in this project and the operational runs was the FDDA initialization. FDDA is not possible when using the Eta PBL scheme. It is critical to compare the two models using the same initialization methods. The AFWA MM5 input files used for all forecasts without FDDA dictated the 21 and 09 UTC initializations opposed to the 00 and 12 UTC standard used by AFWA. This presented an inconsistency in forecast valid times. An AFWA 00 UTC 6-hour forecast is valid at 06 UTC, while a 21 UTC 6-hour forecast is valid at 03 UTC. The final statistics computed present an added bonus of exposing the benefit (or lack-there-of) of using the FDDA initialization. IMVDIF is vertical moisture diffusion in clouds which was also was not possible with the Eta PBL scheme.

Table 2. Model Configuration Comparison.

Configuration	PMM5	MM5	AFWA MM5
Moisture	Reisner 1 (mod)	Reisner 1	Reisner 1
Cumulus	Grell	Grell	Grell
PBL	Eta (mod)	MRF	MRF
Radiation	CCM2 (mod)	Cloud	Cloud
IMVDIF	no	yes	yes
Initialization	cold-start	cold-start	FDDA
Landuse Data	USGS (mod)	USGS	USGS

3.4.1. Model Domain. The parent and nested domains used in these forecasts were required to match the AFWA domains in order to use the same input files. Figure 9 shows the domain over Alaska. Table 3 provides the specific domain configuration parameters. It is important to note that the inner domain contains very little oceanic area that freezes over in the winter. For the period of the forecasts in this project no sea ice was present. The value of adding the sea ice land surface type was therefore not accounted for in this study.

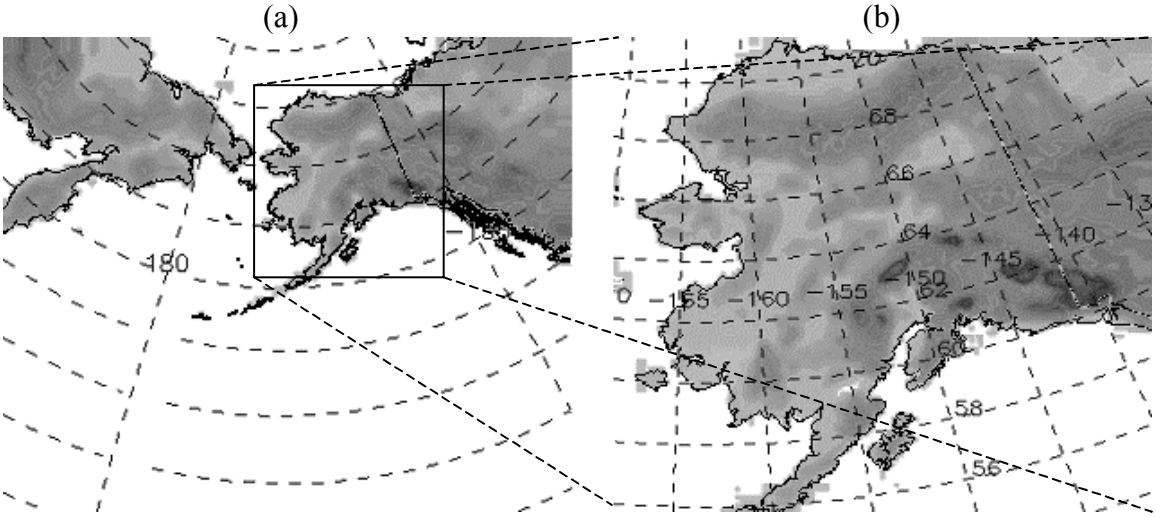

Figure 9. Model Domains. (a) The outer domain with a 45km resolution. (b) The inner domain with a 15km resolution.

Table 3. Universal Model Domain Configuration.

Parameter	Outer Domain	Inner Domain
Horozontal Resolution	45 km	15 km
Vertical Resolution	41 sigma levels	41 sigma levels
Grid Size (N-S x E-W)	97 x 116	97 x 115
Nested Position (NESTI, NESTJ)	-	55,52
Central Latitude	55.8 N, 163.5 W	-
Terrain Resolution	10 min	5 min
Timestep	90 s	30 s
Forecast Length	27 hr	27 hr
Radiation Calculation Frequency	30 min	30 min

3.4.2. Computing Architecture. The model forecasts were computed on an IBM SP P3 supercomputer residing at the MSRC. The first September dataset was initially run on the AFIT meteorology lab network of Sun workstations. A comparison of computing architecture showed lowest sigma level temperature differences between 0.01 K and 0.2 K. These differences are well within the accuracy of the observational measurements as to conclude the difference is negligible.

It was imperative to be frugal with the relatively small amount of processor time (3000 hrs) made available for this project. A few experimental runs provided some computational expense figures to determine the most efficient configuration of processors. Table 4 shows the comparison of processor expense. The value added by doubling the number of processors did not result in a significant reduction in run time. The most cost-effective number of processors was found to be 16, and was used for all the model runs. The orientation of the 16 processors was found to make dramatic impacts on the run time. Optimal efficiency was found with a configuration of 2 processors for the north/south dimension and 8 processors for the east/west dimension.

Table 4. Processor Expense (average time to calculate each timestep (s)).

IBM SP SP3				
# of processors	PMM5		MM5	
	Outer	Inner	Outer	Inner
16	1.712	1.336	1.255	1.137
24	1.21	0.934	0.876	
48	-	-	0.514	0.426
Sun Ultra 10/80				
1	18.333	17.87	20.267	18.432
2	17.178	14.037	11.778	10.333

There were also three versions of compilations to choose; 1) a single processor executable; 2) an Open Multiprocessor (OMP) version and; 3) a multiprocessor instruction (MPI) version. A few results on the Sun architecture showed no differences between the output generated by the three versions. This was in agreement with results from other AFIT students. The MPI version was the version successfully compiled on the IBM.

3.5. Verification Procedure

3.5.1. Verification Overview. The model output required extensive post-processing to achieve a statistical measure of accuracy. The process began with extracting the parameters to be verified from the MM5 output with the use of RIP. The extracted model values were compared to observed ground station and RAOB data for verification. The specific stations used for verification were kept consistent with the AFWA verification process to ensure the validity of the comparison. There are 71 verification surface stations within the inner domain used by AFWA, which are passed through a climatological quality control routine to avoid using bad data. The list of stations may change slightly for each model run. The major departure in processes is that the list of verification stations used by AFWA is dynamic and the surface verification station list used in this project consisted of the same 71 stations for each model run.

An inverse-weighted linear interpolation technique is used in the verification process. This grid-to-station method calculates the model value at the exact station location on the model grid. The closest grid point to the station received the greatest influence over the three other surrounding grid points. Appendix B provides a description of the interpolation

process. The same horizontal interpolation process is duplicated for the surface and upper-air verifications.

3.5.2. Surface Verification Process. The RIP data processing program is used to extract the lowest sigma level parameters of temperature, pressure, east-west wind component, and north-south wind component. The lowest sigma level is located at 20 m AGL. The surface observations are taken in a standardized manner at 2 m AGL. A cursory check against the model ground temperature values proved that it was inappropriate to verify ground temperature against the observation. The ground temperatures were drastically higher than the observations. The lowest sigma level values of temperature and wind were used to be consistent with the AFWA verification process.

A correction factor was applied to reduce the lowest sigma level model pressures down to the model surface. A hydrostatic approximation was applied to the height difference of 18 m (from lowest sigma level to observation level). This was found to be a correction factor of 2.16 mb. The verification procedure was calculated at every 3-hour period through the 27-hour prediction.

The residuals were calculated as,

$$\text{residual} = \text{model} - \text{observation}. \tag{5}$$

This residual convention allows for an interpretation of a positive residual as a model over-prediction. The residuals for each station are averaged for all 21 UTC runs and all 09 UTC runs separately. The overlapping of 21 and 09 UTC forecast periods resulted in a violation of dependence, especially for a small sample size. The separation of 21 and 09 UTC runs was made to alleviate statistical errors inherent in data dependence.

The basic statistical parameters of root mean square error (RMSE) and bias were calculated following Wilkes (1995). Bias was calculated as the arithmetic mean of the sample of n residuals. RMSE was calculated by equation 6.

$$\mathrm{RMSE} = \sqrt{\frac{\Sigma(\mathrm{predicted} - \mathrm{observed})^2}{n}} \tag{6}$$

Predicted and observed represent the individual meteorological parameters. N is the number of valid observations summed to obtain the average.

Root mean square vector error (RMSVE) was used to verify the model generated wind field. RMSVE was chosen in an effort to simplify the results opposed to analyzing direction and speed separately. RMSVE takes both speed and direction into account and is calculated by equation 7.

$$\mathrm{RMSVE} = \sqrt{\frac{\Sigma\left[\left(u_{pred} - u_{obs}\right)^2 + \left(v_{pred} - v_{obs}\right)^2\right]}{n}} \tag{7}$$

The east-west and north-south wind components are represented by u and v respectively. Model predicted components are denoted by the subscript pred, and observed components are denoted by the subscript obs. The value of n is the number of wind observations (i.e. valid reporting stations) summed to obtain an average at a specific forecast hour for the domain RMSVE.

If the wind speed between the model and observation are in close agreement but the wind directions are not, RMSVE will take on a high value. The predicted wind speed and direction must closely match the observation to produce a low RMSVE. RMSVE takes on positive values, with zero representing a perfect forecast. The units of RMSVE are m s^{-1}, but

are not necessarily the magnitude of the speed error. The squaring of the components to arrive at an error resultant vector excluded a measure of bias.

The goal of this project is to compare these statistical measures of RMSE and bias by analyzing the following difference,

$$\Delta = \text{MM5} - \text{PMM5}. \tag{8}$$

This difference is consistent for all comparisons, therefore a positive value of Δ for RMSE can be interpreted as a greater verification error produced by the MM5 than the PMM5.
A paired *t*-test was conducted to identify statistically significant differences between the two models at a 95% confidence level. The computations were made following Wilkes (1995). The null and alternative hypotheses were respectively,

$$H_o: \ \Delta = 0 \tag{9}$$

$$H_a: \ \Delta \neq 0 \tag{10}$$

The significance paired *t*-test results were also calculated with SAS Institute Inc. JMPIN v.4.0.2. for computational assurance.

Statistics were also computed for each station individually to achieve an assessment of the spatial distribution of model accuracy. These station-specific statistics represent a RMSE and a bias for each station over all model runs for each forecast time. A regional assessment of error was analyzed by grouping the stations into three climatologically separated regions depicted by Figure 10. This separation into three regions accomplishes a further assessment of the comparison of the PMM5 and MM5 as well as highlighting model accuracy/biases specific to the regions.

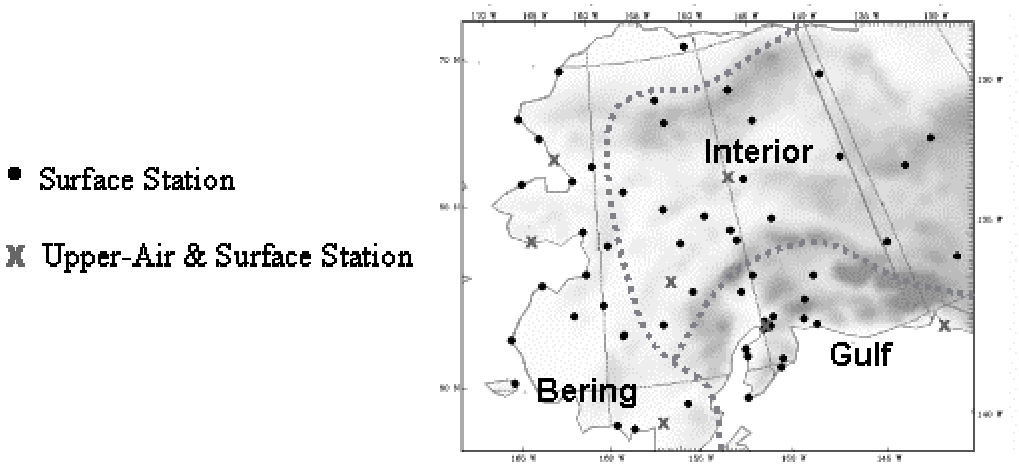

Figure 10. Distribution of Verification Stations. Dashed line defines the three climatologically distinct regions, Bering Sea, Gulf of Alaska, and the Interior Regions overlaid on the relief map of Figure 1.

3.5.3. Vertical Verification Process. RIP is used to extract vertical parameters of geopotential height, pressure, temperature, and water vapor mixing ratio. Each of the vertical parameters is interpolated for each of the seven RAOB reporting stations. Table 5 lists the stations used for the vertical verification. The RAOB data contained all mandatory and significant levels, which varied for every station and every observation.

Table 5. Upper-Air Verification Stations.

Station	ICAO	Latitude (N)	Longitude (W)	Elevation (m)
Anchorage	PANC	61.17	150.02	40
Fairbanks	PAFA	64.82	147.87	132
King Salmon	PAKN	58.67	156.64	15
Kotzebue	PAOT	66.86	162.62	5
Mcgrath	PAMC	62.96	155.62	103
Nome	PAOM	64.52	165.45	11
Yakutat	PAYA	59.51	139.67	9

The horizontally interpolated model data are subtracted from the vertically logarithmic-linear interpolated RAOB data to arrive at residuals on the same sigma level. The RAOB observation heights were converted to geopotential height assuming a hydrostatic approximation following List (1984). Dew point temperature reported from the RAOB was converted to relative humidity following Wallace and Hobbs (1977).

3.6. Terrain Analysis

The process of verifying near-surface parameters is highly influenced by the topography. The extreme slope of mountainous regions, isolated pinnacles, and sharp valleys are examples of sources of error in terrain analysis used in the model. The inner domain contains a very diverse distribution of topography ranging from the highest point in North America (Denali 6193.5 m) to more coastline than all of the Contiguous 48 States. This warranted a crucial assessment of the accuracy of the terrain grid used in the forecasts.

The same interpolation and statistics routines that were used to compute the horizontal verification results were applied to the model terrain grid (in tenths of meters). The residuals were consistently higher than the actual station elevations (in meters). It became imperative to exclude certain stations exceeding a residual criterion. Figure 11 shows the histogram of terrain residuals.

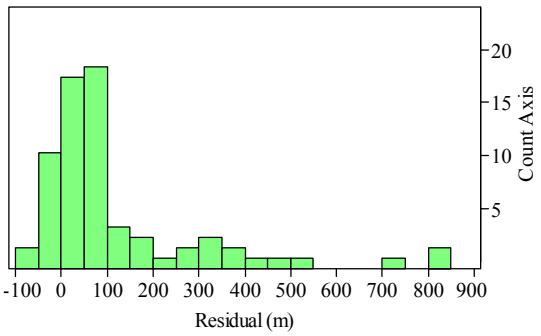

Figure 11. Distribution of Terrain Residuals.

The distribution of lowest sigma level temperature residuals was analyzed to determine a residual criterion to exclude verification stations. This distribution should ideally compare to a terrain residual distribution. It was found that approximately 99% of these temperature residuals were less than 3.5 K. This was defined as the acceptable range of

error based on a dry adiabatic lapse rate. Assuming this lapse rate of 10 K/1000 m, 3.5 K corresponds to a residual criterion of 350 m. Eight station locations with an absolute value of terrain residual greater than 350 m were excluded from the verification process. Table 6 displays the computed statistics against the actual station elevations for all 71 stations and with the eight bad stations removed. Similar findings by Manning and Davis (1997) found the general model terrain to be too high as a result of the smoothing of the grid resolution.

Table 6. Terrain Analysis Statistics.

Parameter	**All 71 Stations**	**63 Stations with residual < 350 m**
Correlation	0.22	0.83
RMSE	226.39 m	114.71 m
Bias	125.82 m	70.05 m

Slope was another analyzed feature of the model terrain grid using an arbitrary criterion of a 60° slope defining excessive terrain grade. A range criterion of two grid distances (30 km) from a point of excessive slope was established and it was found that no stations were within this criterion of 60° slope. This is further evidence that the widely varying terrain found in the Alaskan domain is not represented well enough at a horizontal resolution of 15 km.

IV. Analysis of Results

4.1. Overview

This chapter presents the finding of this research, focused on the difference between the PMM5 and MM5. The difference has been consistently applied as the MM5 values minus the PMM5 values. The sample sizes are 34 – 21 UTC runs and 33 – 09 UTC runs. Computer resources and research time limited these sample sizes. The statistical results of RMSE and bias are generally consistent with other previous work with the PMM5 by Bromwich et al. (2001b), and resemble the patterns of AFWA real-time verification statistics. This lends credibility to these results even with a relatively small sample size.

The surface observations reported by manual observers and by automated surface observation stations (ASOS), along with the RAOBs, are treated as the 'ground truth'. Table 7 lists the average accuracies of the sensors used to make the surface and upper-air observations. These accuracy figures ultimately determine the significance of the model differences. Table 7 was constructed from sensor information published for a variety

Table 7. Observation Sensor Accuracies.

Surface Observations	
Parameter	Sensor Accuracy
Temperature	± 1.0 K
Pressure	± 0.5 mb
Wind Speed	± 1 m s^{-1}
Wind Direction	± 5 º

Upper-Air Observations	
Parameter	Sensor Accuracy
Temperature	± 0.2 K
Pressure	± 0.5 mb
Humidity	± 3 % RH

of instrumentation used in Alaska by Mannarano (1998), Vaisala (2002), Department of the Air Force (1994, 1997, and 1998). The sensors include the Automated Surface Observing System (ASOS), Vaisala RS80-57 radiosondes, and a variety of standardized equipment used on the Air Force Bases in Alaska.

A quality control routine was applied to these observations to remove unrealistic values. Unrealistic values were temperatures above 100 C, pressures above 1040 mb, and winds above 100 knots. The assessment of the results by-station allowed for an in-depth analysis of the residuals. This in-depth analysis highlighted outliers that would have been hidden by focusing solely on the domain averages. The term 'error' is used to describe RMSE and bias interchangeably unless explicitly stated.

4.2. Validation of Replicating AFWA Operational Methods

This section compares the MM5 runs made in this research to the operational MM5 run and verified at AFWA. A comparison of verification procedures is also presented. The verification results from the control MM5 are compared to the operational verification results published by AFWA. The FDDA initialization used by AFWA is not possible with the Eta PBL scheme used in the PMM5 as described in section 3.4. This warranted making MM5 forecasts separate from the AFWA operational runs. The results in this section comparing AFWA procedures to the experiment procedures of this project provide limited value for three reasons:

1. Initialization time inconsistency. The model runs in this experiment could not be initialized at the standard 00 and 12 UTC times as a result of using MM5 input files configured for FDDA (containing data for the previous three

hours). This results in different valid times for the same duration forecast for the control MM5 and the AFWA MM5. An AFWA 00 UTC 6-hour forecast is valid at 06 UTC, while a 21 UTC 6-hour forecast is valid at 03 UTC.

2. The AFWA statistics used in the upper-air comparisons are verification results from the **outer** domain, containing double the verification stations of the inner domain verified for the control MM5 results.
3. The AFWA statistics are averaged over many more runs from September through November, where the control MM5 statistics are only for the 67 runs from September through December.

Figure 12 is a plot of the RMSE and bias differences (AFWA-Control) between the models. The AFWA statistics were calculated from AFWA MM5 output data by the same verification routine used for the control MM5 statistics. The bottom axis represents the valid hour (UTC) of the forecast, opposed to forecast duration. The inconsistency in initialization time prohibited plotting against forecast hour, as the two models are valid at different times. The result differences arising from the different initialization times and methods (FDDA vs. cold-start) are all less than 0.5 K. This small difference falls within the measurement accuracy of ±1 K, justifying the premise that the two models are identical.

Computational problems arose that made a comparison of MSL pressure statistics unavailable for the AFWA MM5. Figure 13 presents similar results for surface wind RMSVE between the AFWA MM5 and control MM5. Again, these model error differences were found to fall well within the accuracy of the measurement and can be assumed to be equal.

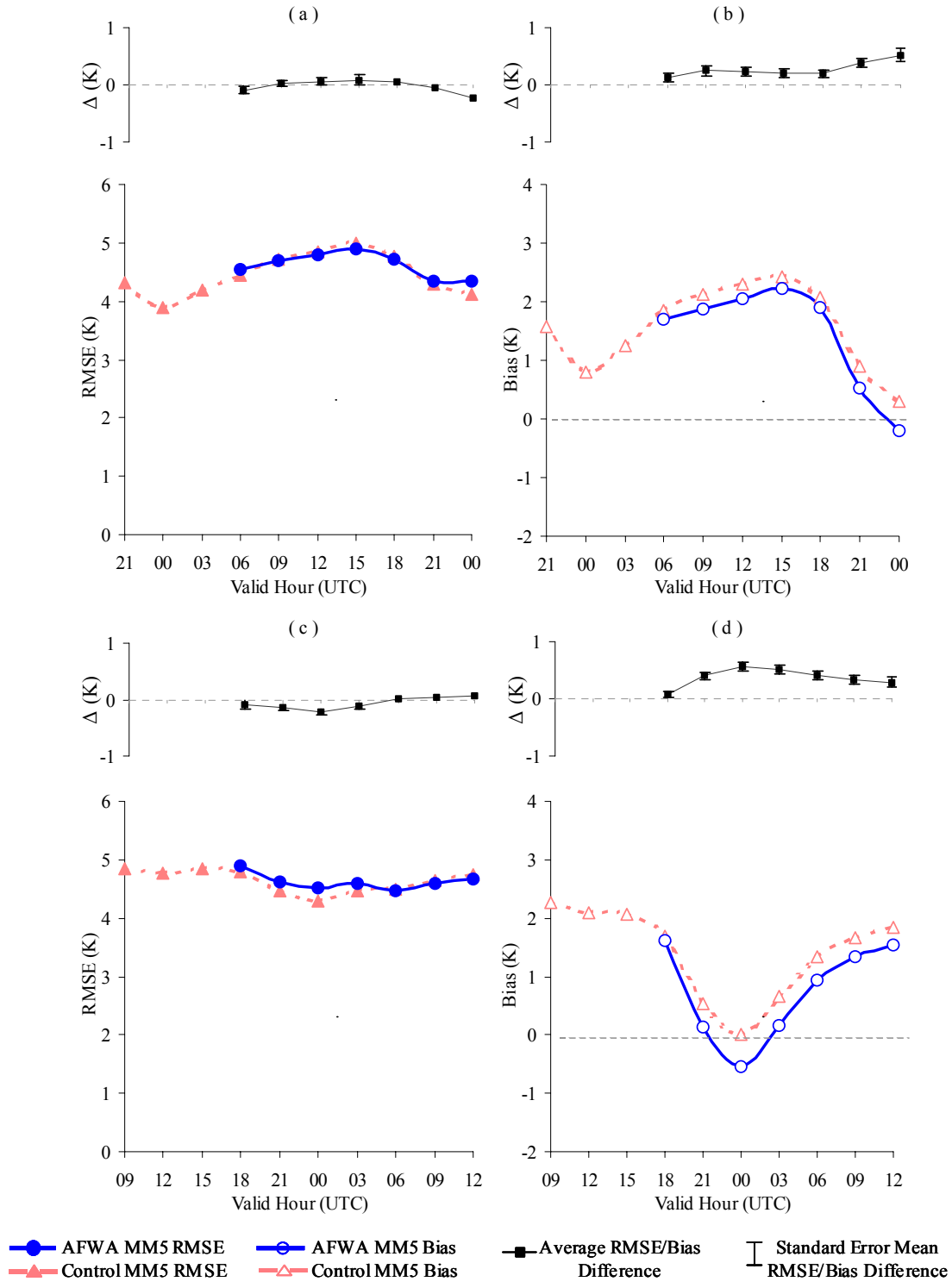

Figure 12. AFWA MM5 and Control MM5 Surface Temperature Comparison. (a) 00 UTC AFWA and 21 UTC Control RMSE, (b) 00 UTC AFWA and 21 UTC Control Bias, (c) 12 UTC AFWA and 09 UTC Control RMSE, (d) 12 UTC AFWA and 09 UTC Control Bias. Results are plotted by VALID time, not forecast integration time.

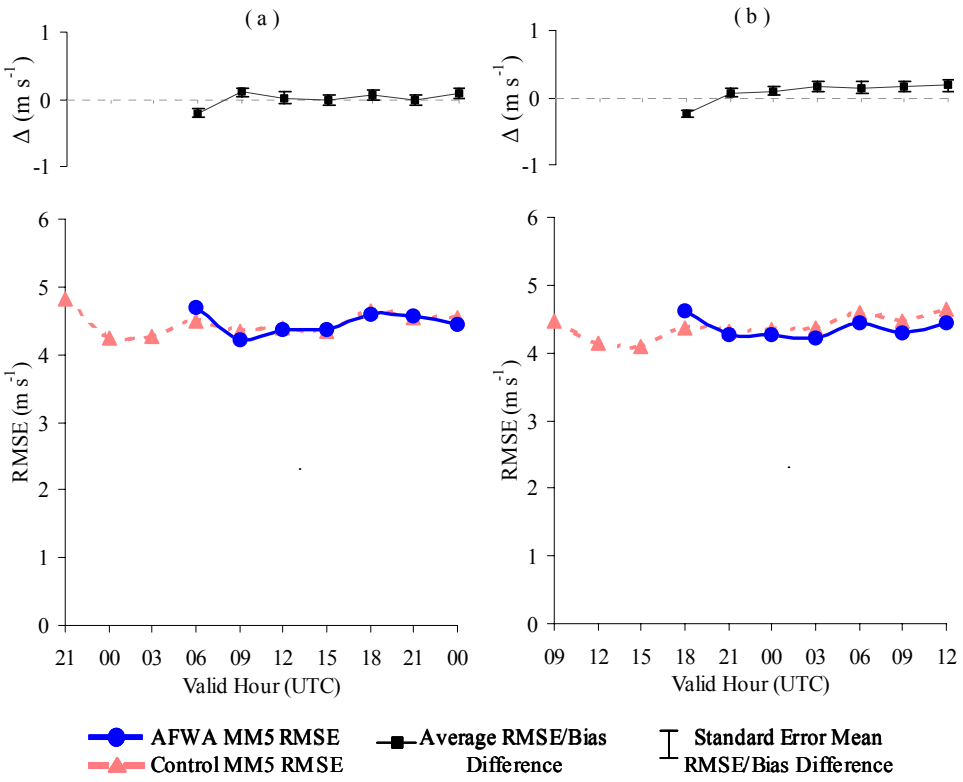

Figure 13. AFWA MM5 and Control MM5 Surface Wind Comparison. (a) 00 UTC AFWA and 21 UTC Control RMSVE, (b) 12 UTC AFWA and 09 UTC Control RMSVE. Results are plotted by VALID time, not forecast integration time.

The domain, initialization time, and verification method inconsistencies of the upper-air comparisons between the AFWA and control MM5 runs of this project can explain the subtle differences. The actual values of difference can therefore not be considered however, assumptions can be made based on the trends of the two models. The AFWA upper-air values are operational real-time verification statistics published for the outer domain for Fall 2001. The statistics were calculated from 14 observation sites by AFWA's verification procedure on the mandatory levels of 1000, 925, 850, 700, 500, 400, 300, 250, and 100 mb. Figure 14 depicts the temperature relationship between the AFWA MM5 and the control MM5. The same maxima and minima features are found in both MM5 forecasts, but the

AFWA version shows slightly greater extreme bias values. These bias discrepancies can be attributed to the greater variations possible based on more stations in the larger domain.

Geopotential height trends are compared in Figure 15. The bias trends are very similar and lend credibility to the assumption of equating the models. Figures 15 (b) and (c) show a departure in RMSE trend in the upper atmosphere. The control MM5 exhibits RMSE

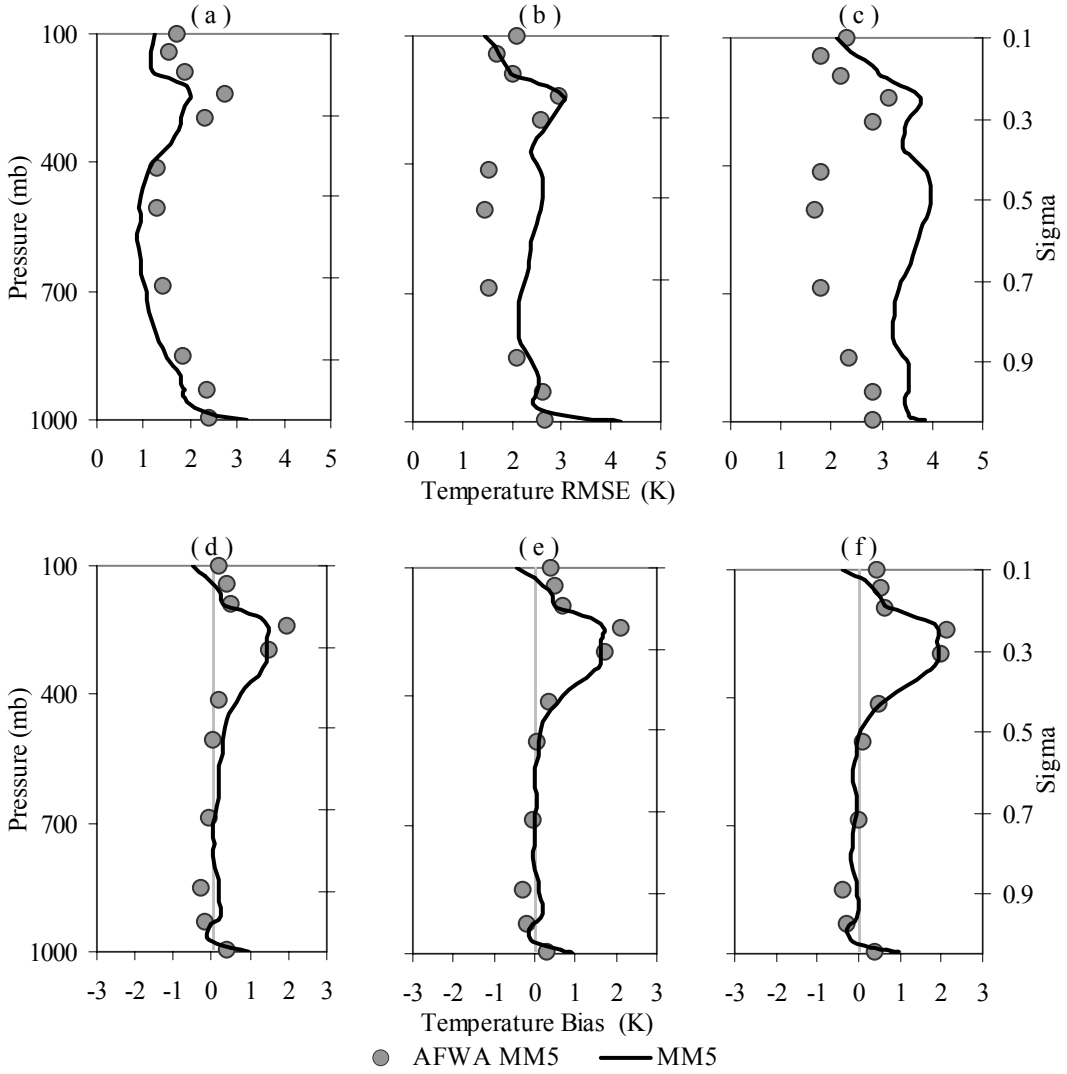

Figure 14. AFWA MM5 and Control MM5 Upper-Air Temperature Comparison. The AFWA MM5 results are averaged verifications from the outer domain initialized at 00 and 12 UTC. The control MM5 results are averaged verifications from the inner domain initialized at 21 and 09 UTC. (a) & (d) 00-hour (AFWA), 03-hour (control MM5) forecasts; (b) & (e) 12-hour (AFWA), 15-hour (control MM5) forecasts; (c) & (f) 24-hour (AFWA), 27-hour (control MM5) forecasts.

maxima around 300 mb in both 15-hour and 27-hour forecasts. The AFWA response is a continual increase through the tropopause. These temperature and geopotential height upper-air charts show that there is no appreciable bias trend divergence between the AFWA MM5 and the control MM5. The large differences in RMSE can be partially accounted for by the fact that RMSE places greater weight to larger errors as a result of the squaring of the residuals. The control MM5 can be treated as equivalent to the AFWA operational MM5,

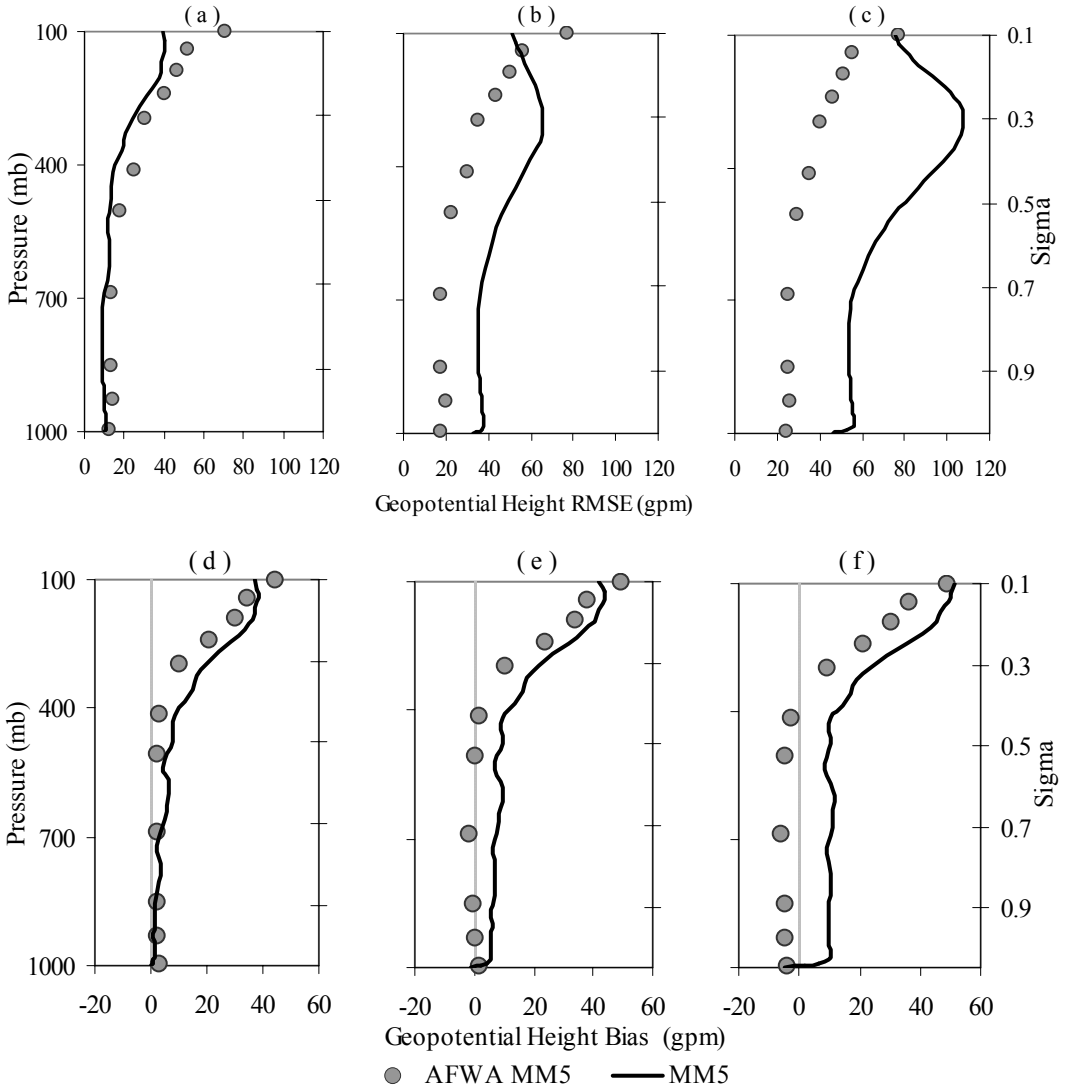

Figure 15. AFWA MM5 and Control MM5 Upper-Air Geopotential Height Comparison. The AFWA MM5 results are averaged verifications from the outer domain initialized at 00 and 12 UTC. The control MM5 results are averaged verifications from the inner domain initialized at 21 and 09 UTC. (a) & (d) 00-hour (AFWA), 03-hour (control MM5) forecasts; (b) & (e) 12-hour (AFWA), 15-hour (control MM5) forecasts; (c) & (f) 24-hour (AFWA), 27-hour (control MM5) forecasts.

based on the small differences in surface errors and the consistent trends in upper-air biases. Another comparison is required to analyze the differences in verification sequences between AFWA and that implemented in this research.

A comparison of verification routines was necessary to ensure the AFWA process was consistent with the process used in this study. This comparison was achieved by putting the AFWA MM5 output through the verification routine used in this project and graphed against the verification statistics computed by AFWA from the same MM5 output. These statistics were calculated from the inner domain initialized at 00 UTC and 12 UTC for all 67 runs of the experiment. This AFWA MM5 output was not available until the 6-hour point in 3-hourly increments. The AFWA statistics were calculated for the outer domain from the Fall 2001 runs in 6-hourly increments. Figure 16 compares the 00 UTC (a) and 12 UTC (b) AFWA MM5 outer domain statistics to the results of the inner domain from the verification routine used in this research by forecast hour. The value of this comparison shows that the two verification routines are in relative agreement. Therefore, the assumption is made that

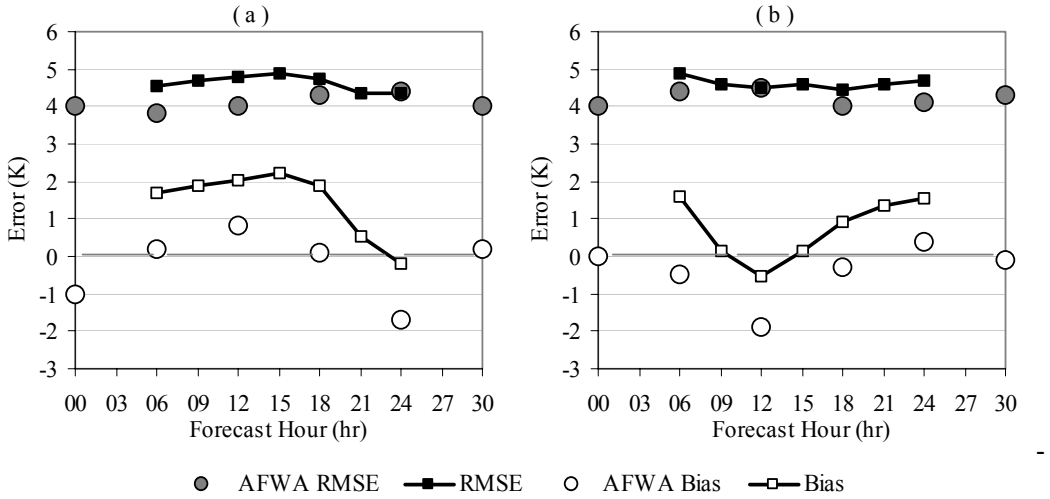

Figure 16. Verification Routine Comparison. (a) Verification of surface temperature for (a) 00 UTC AFWA MM5 runs and (b) 12 UTC AFWA MM5 runs. AFWA values are outer domain results calculated by the AFWA verification routine. Generic RMSE and Bias are calculated by the verification routine used in this research for the inner domain.

the verification results calculated in this project duplicate the results of the AFWA verification process. The validation that the control MM5 can be assumed to represent the AFWA MM5, and that the verification process used in this project produces results consistent with the AFWA verification process provides the foundation for comparing the PMM5 to the control MM5.

4.3. Surface Temperature Verification Results

The results of RMSE and bias are presented in Figure 17. The bottom axis represents the forecast integration time at each 3 hourly period that model output was generated. The black bars represent the results of the paired *t*-test. The presence of a black bar denotes that the P-value was less than or equal to the type-I error level (α) of 0.05. These represent forecast hours where the null hypothesis, H_o: $\Delta=0$, was rejected. The absence of a black bar represents a forecast hour where the differences between the model parameters were not significant enough to declare a statistically significant difference. It is important to not conclude that these are areas where the two models are the same, but rather that there is not enough evidence to prove they are different. The α-level chance that a test is wrong is inherent in the paired *t*-test; in this case a 5% chance. The required assumption of normality was violated (by Shapiro-Wilk test) in a few of the distributions of differences at certain forecast hours. These occurrences were rare, and explain the few inconsistencies in some of the significance tests results.

Figure 17 (a) shows the gradual increase in error throughout the forecast integration, which is expected as a forecast gets worse over time. The difference between the models RMSEs gradually decreases through the 18-hour forecast. The significance tests

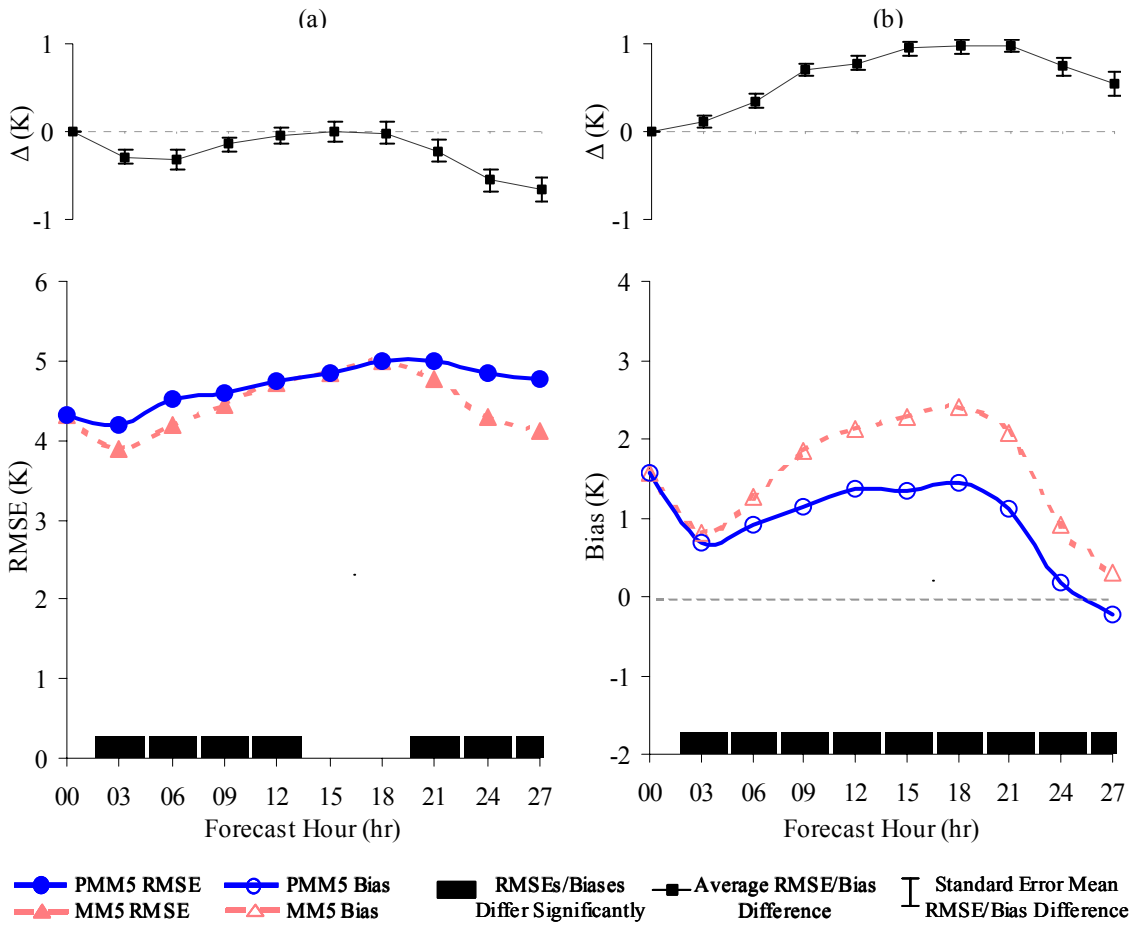

Figure 17. 21 UTC Initialization Surface Temperature Verification Results. (a) RMSE of PMM5 and MM5, (b) Bias of PMM5 and MM5. The top graphs of Δ represent the average differences (MM5-PMM5) and the standard error mean of the distribution of differences used in the significance test.

provide an accurate depiction of where the differences between the models are significant. The areas where the standard error of the mean crosses zero can be interpreted as areas where the models do not differ significantly.

Figure 17 (b) shows the diurnal curve of temperature bias. The relative maxima in biases occur at the time of minimum temperature for these 21 UTC initialization forecasts. This initialization time corresponds to a local time of 1200 Alaska Standard Time (AST). The broad maxima occur around 03-06 AST. The increase in bias corresponds to the smaller increase in RMSE, representing a particular model difficulty in forecasting minimum

temperature. The PMM5 produces greater RMSE values than the MM5 in general however, the lower PMM5 biases were more significantly different from MM5 biases. The lower (closer to zero) bias of the PMM5 with a greater RMSE (than the MM5) suggests that there is more variance in the PMM5 residuals. This could be characterized by a more physically realistic solution of the PMM5 than the MM5. This theory would require further analysis of the horizontal features beyond the scope of this project to validate.

Figure 18 presents the identical statistics as Figure 17 but for an initialization time of 09 UTC, or 0000 AST (midnight). The diurnal patterns of the maximum temperature time are the inverse of the 21 UTC forecast minimum temperature patterns. The marked decrease (closer to zero) in bias at 15 UTC, or 1500 AST show that the models have an easier time forecasting maximum temperature from a 09 UTC run than forecasting minimum

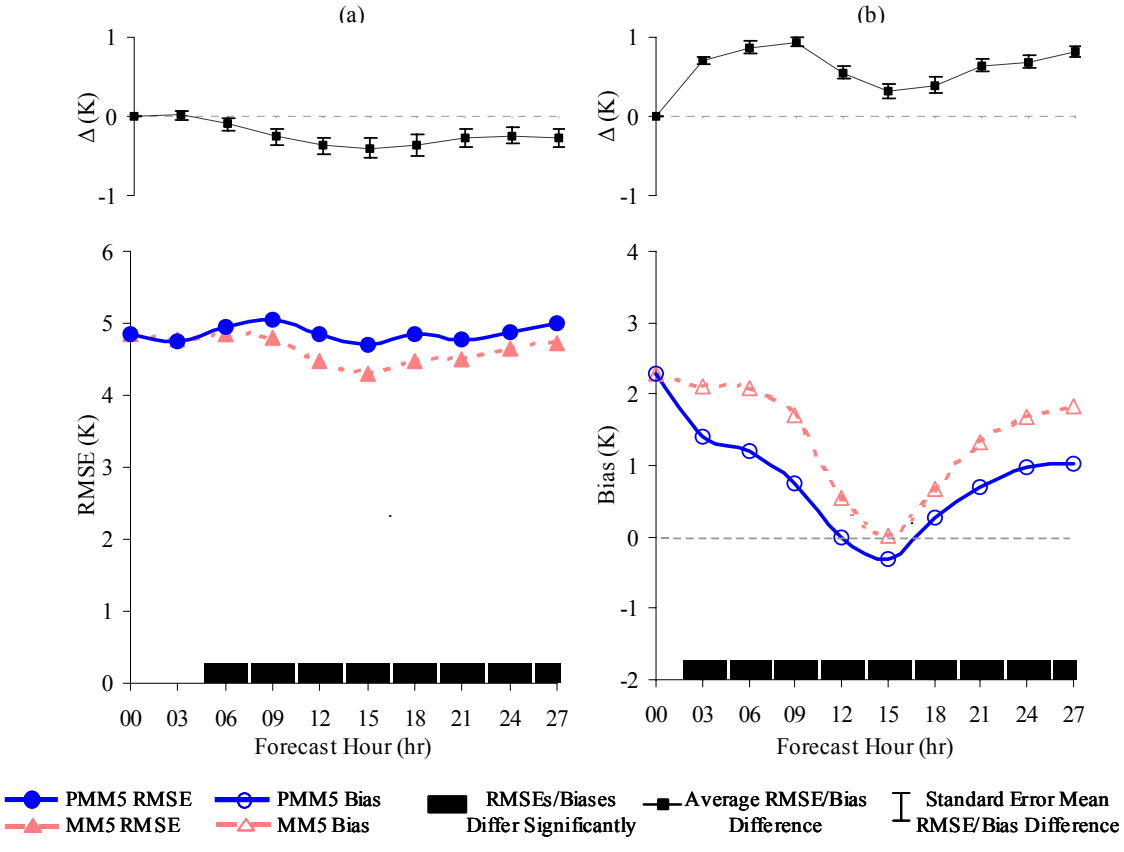

Figure 18. 09 UTC Initialization Surface Temperature Verification Results. Same as Figure 17

temperature from a 21 UTC run. The slight decrease in RMSE for the same forecast period supports this finding. This diurnal pattern is evident in the longer forecast. Figure 19 shows RMSE and bias results of both 00 UTC and 12 UTC operational runs from the AFWA MM5.

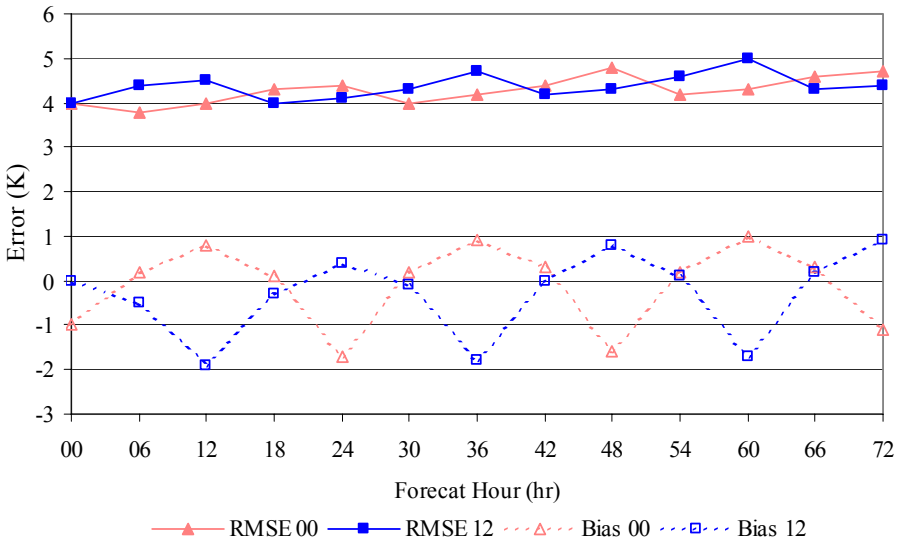

Figure 19. AFWA Temperature Verification for the Alaska Outer Domain. Data compiled from Fall 2001 forecasts.

The 21 and 09 UTC model runs show that the domain RMSE for the PMM5 is always greater than the RMSE for the MM5. The PMM5 biases are consistently smaller than the MM5 biases. The paired *t*-tests show that these differences are almost always significant, the magnitude of which becomes an important focus. The average RMSE difference is –0.22 K and the average bias difference is 0.60 K, which fall within the average accuracy of the temperature sensors of ±1 K. Analysis of the individual station statistics (by-station) provides more detail in explaining the root of these differences.

4.3.1. By-Station Surface Temperature Analysis. The RMSE and bias were calculated for each station over all forecasts at each 3 hourly forecast period. These by-station results were grouped into the 3 respective regions defined by Figure 10. This

grouping provides a method of distinguishing a spatial relationship of the error in contrast to analyzing the entire domain. Figure 20 is a representative example of the typical distribution of error in the domain. The gaps represent stations missing observations for the valid time or stations excluded by exceeding the terrain criteria discussed in section 3.6. Several trends are noticeable in Figure 20 that would not be evident by simply analyzing the domain averages. The trends depicted in Figure 20 are very consistent throughout nearly all forecasts and forecast hours.

The average error of both models in the Interior Region is noticeably greater than in the other regions. The PMM5 RMSE is greater than the MM5 RMSE for nearly every station in the Interior. The PMM5 produced smaller RMSE values than the MM5 for most stations in the other two regions. The stations with greater PMM5 RMSE were consistent for all forecast hours of each run. The magnitude of the differences in the Interior was large enough to influence the domain average difference, resulting in the overall greater PMM5 error.

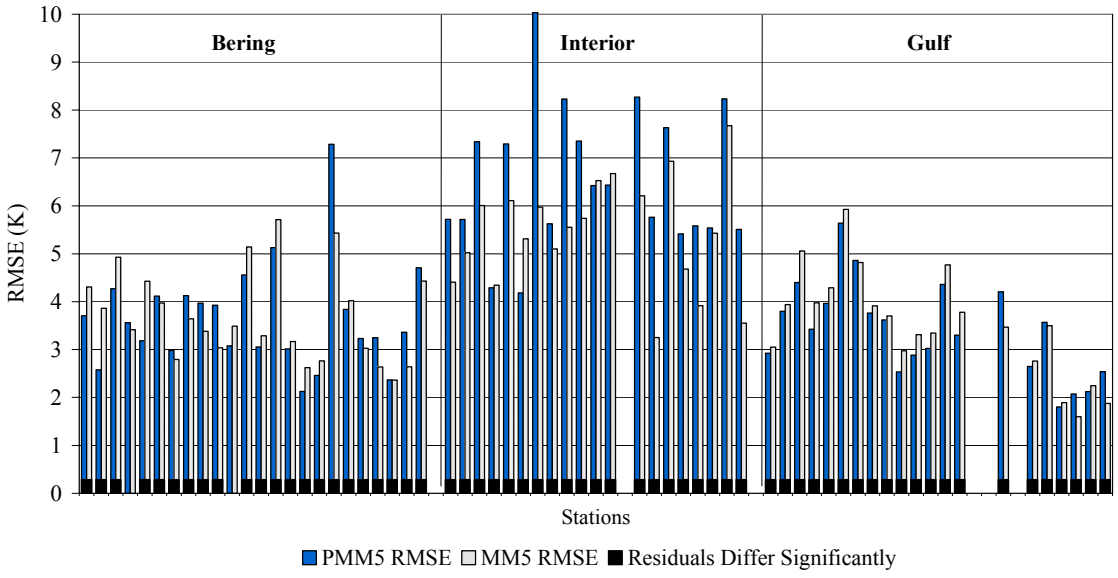

Figure 20. By-Station Surface Temperature RMSE. 09 UTC initialization 15 hour forecast.

Figure 21 is a by-station breakdown of temperature bias to make an assessment of the differences in error between the PMM5 and MM5. The distribution of error across the stations was not as consistent over all forecast hours for the biases as the RMSEs. Figure 21 is the closest representation of the 20 charts.

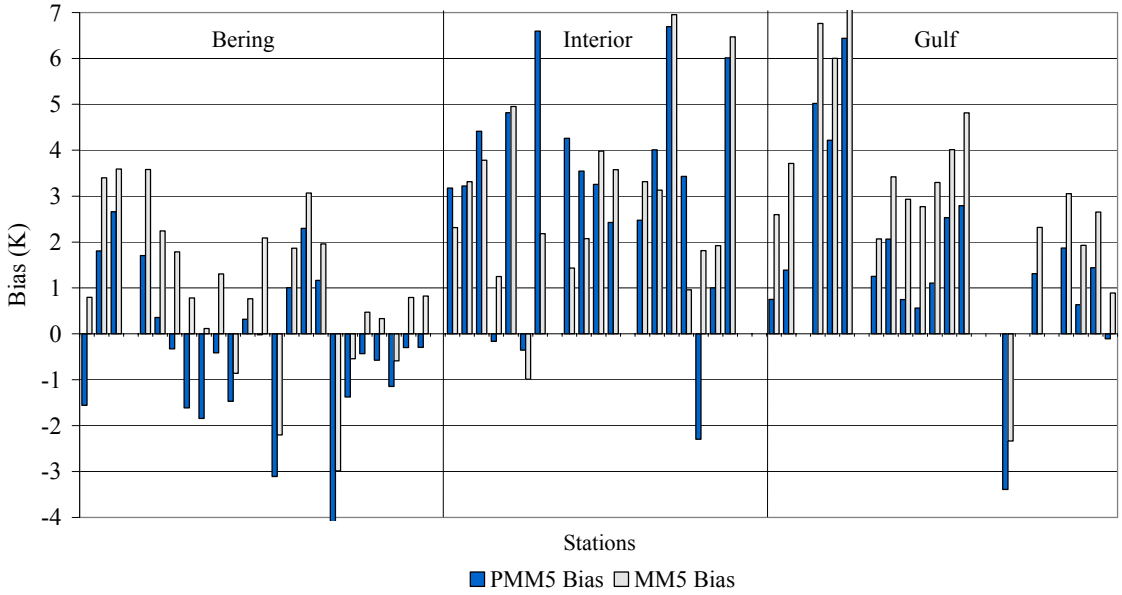

Figure 21. By-Station Surface Temperature Bias. 21 UTC 15 hour forecast.

The station bias trends are similar between the two models, with few exceptions where the biases were opposite in sign. The overall greater error is found in the Interior similar to the RMSE trend. The Bering region contained the greatest amount of difference between the model biases, with the PMM5 producing colder forecasts, while the MM5 produced warmer forecasts. The Gulf and Interior regions contained almost exclusively warmer forecasts than was actually observed. It is apparent that most MM5 station biases are greater than PMM5 station biases, providing reasoning for the higher MM5 *domain* bias.

It can be generally stated that the PMM5 generates cold temperatures in the Bering region, but the excessively warm bias in the other regions overwhelms the average to result

in a domain average positive bias. The MM5 produced a warm bias at almost every station at every forecast hour. This is consistent with the opinion of the operational forecaster, which prompted this research.

4.3.2. Regional Surface Temperature Analysis. The magnitude of the number of charts generated to perform a by-station analysis required a method of summarization. Figure 22 summarizes the RMSE and bias differences between regions of the PMM5 only. The same trends were found in the MM5. The examples shown in Figures 20 and 21 are averaged over each region, for every forecast hour. The Interior RMSE values are nearly 3 K greater than the other two regions. The model has an apparent difficulty in forecasting the continental region of the Interior. The higher biases in the Interior Region correspond to the higher RMSEs in the Interior. The cold bias is evident in the Bering Region with nearly all bias averages below zero in the Bering Region. The higher error of the Gulf Region compared to the Bering Region can be

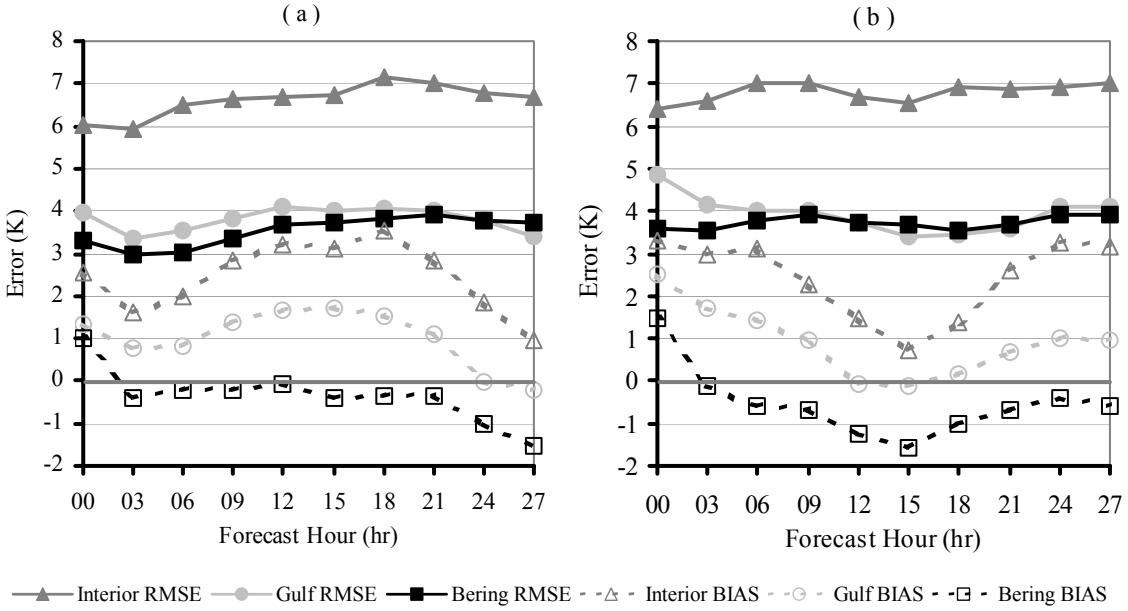

Figure 22. Regional **PMM5** Temperature RMSE and Bias Comparison. (a) 21 UTC initialization averages, (b) 09 UTC initialization averages.

partially explained by the significant terrain found in the Gulf Region, compared to the relatively flat terrain of the Bering region which covers the vast Yukon-Kuskokwim Delta depicted in Figure 1.

The regional differences in model error between the PMM5 and MM5 were found to be significant in magnitude and consistent for all forecast times. The regional RMSE and bias values for the MM5 are differenced from the PMM5 regional values in Figure 22 to find regional differences between the two models. Figure 23 shows the regional model differences (MM5-PMM5) in surface temperature by forecast hour. A positive value denotes a greater MM5 error and a negative value corresponds to a greater PMM5 error. The 09 UTC differences resembled the 21 UTC results. The PMM5 has considerable difficulty with the Interior Region based on the greater RMSE and bias than the MM5 at all forecast times. This provides evidence for future interrogation to determine how the PMM5 modifications affect the model solution. The large differences between the dry continental regime of the

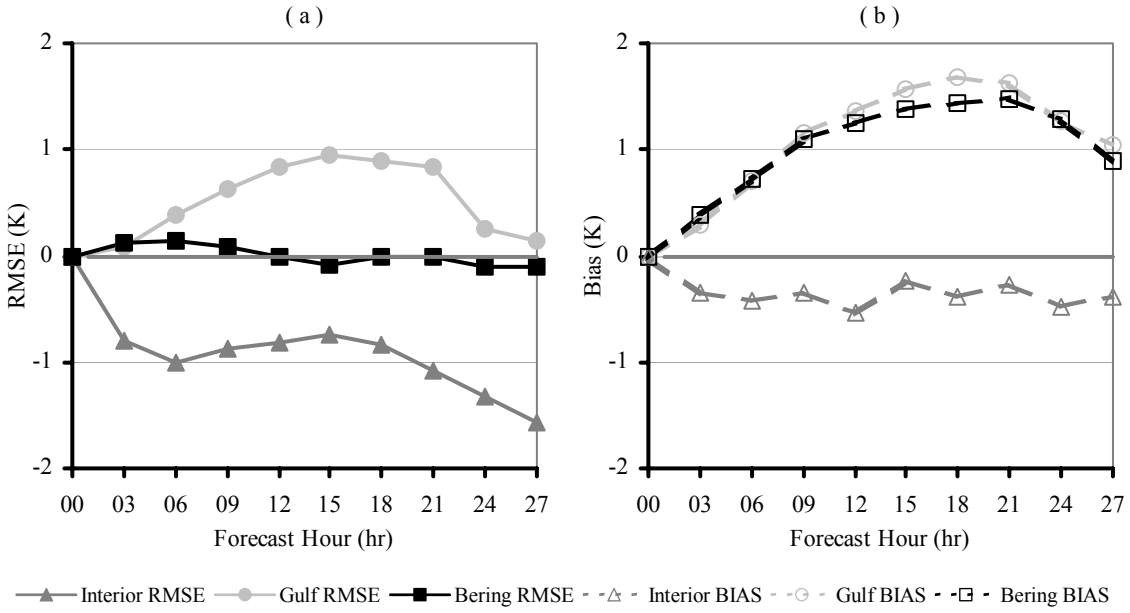

Figure 23. Regional Temperature Model Error Differences (MM5-PMM5). (a) 21 UTC initialization temperature RMSE, (b) 21 UTC initialization temperature bias.

Interior and the more moderate maritime regime of the Gulf may suggest that there is a moisture problem in the PMM5. The PMM5 has overcorrected the warm bias of the MM5 in the Interior, but exacerbated the warm bias of the MM5 in the Gulf Region.

A further analysis of the specific station trends provided new insight not attainable from the previous charts. Figure 24 shows the observed and forecasted values of surface

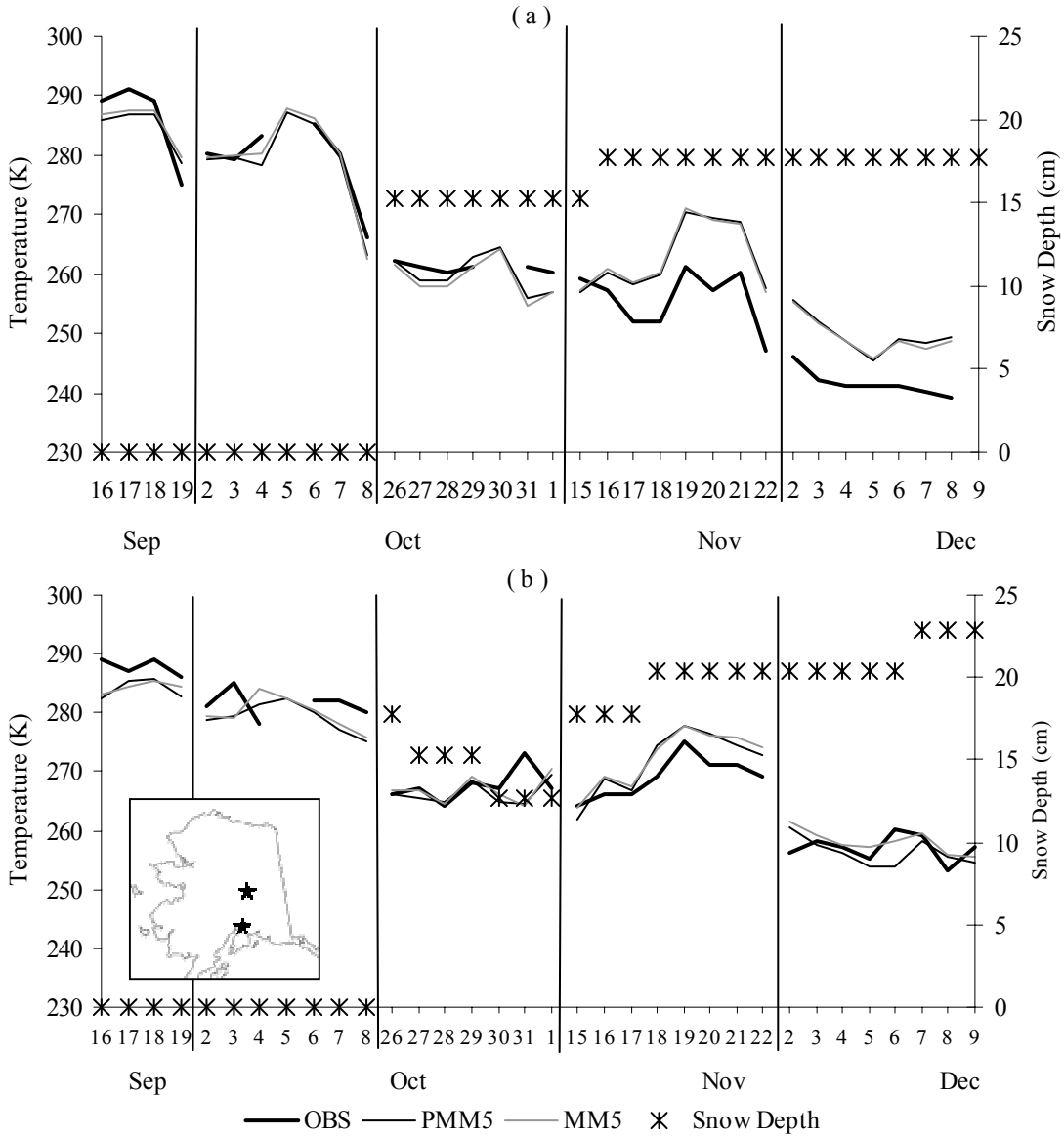

Figure 24. Surface Temperature Observation and Model Trends. 21 UTC 27-hour forecasts and observations for (a) Eielson AFB (northern star), and (b) Elmendorf AFB (southern star) by valid time. Vertical lines denote temporal breaks in forecasts.

temperature for two selected sites, Eielson and Elmendorf AFB. The map inset in Figure 24 (b) shows the location of Eielson AFB (northern star, Interior Region) and Elmendorf AFB (southern star, Gulf Region). The models show a relatively close response to the observations. The greatest errors are apparent at Eielson AFB during a very cold artic outbreak in early December. These significant errors under such extreme conditions substantiate claims from forecasters. The drastic warm bias during this period can be partially attributed to the 18 m height differential between the model value (lowest sigma level height) and the observed height (2 m). It is not uncommon to experience a radiation inversion with a 40-degree (K) temperature change over the lowest 1500 m of the atmosphere during an arctic outbreak. This would induce a warm bias over lesser-extreme conditions. The most significant trends in these figures are the cold biases in the earlier forecasts (fall) compared to the warm biases in the latter forecasts (winter). The exclusion of assimilated snow cover into the model used in both PMM5 and MM5 is a possible cause of this error.

4.4. Mean Sea Level Pressure Verification Results

Mean sea level pressure was calculated from observed altimeter settings to represent the 'ground truth'. The fact that the station elevations and model terrain heights at each station are not equal introduces a possible bias to the verification results. The goal of this research is to examine the differences between these verification results. This potential bias exists identically in both MM5 and PMM5 verifications and therefore is irrelevant when analyzing the differences between the two models. Figure 25 (next page) shows the RMSE and bias results for surface pressure averaged over all the 21 and 09 UTC initialized model

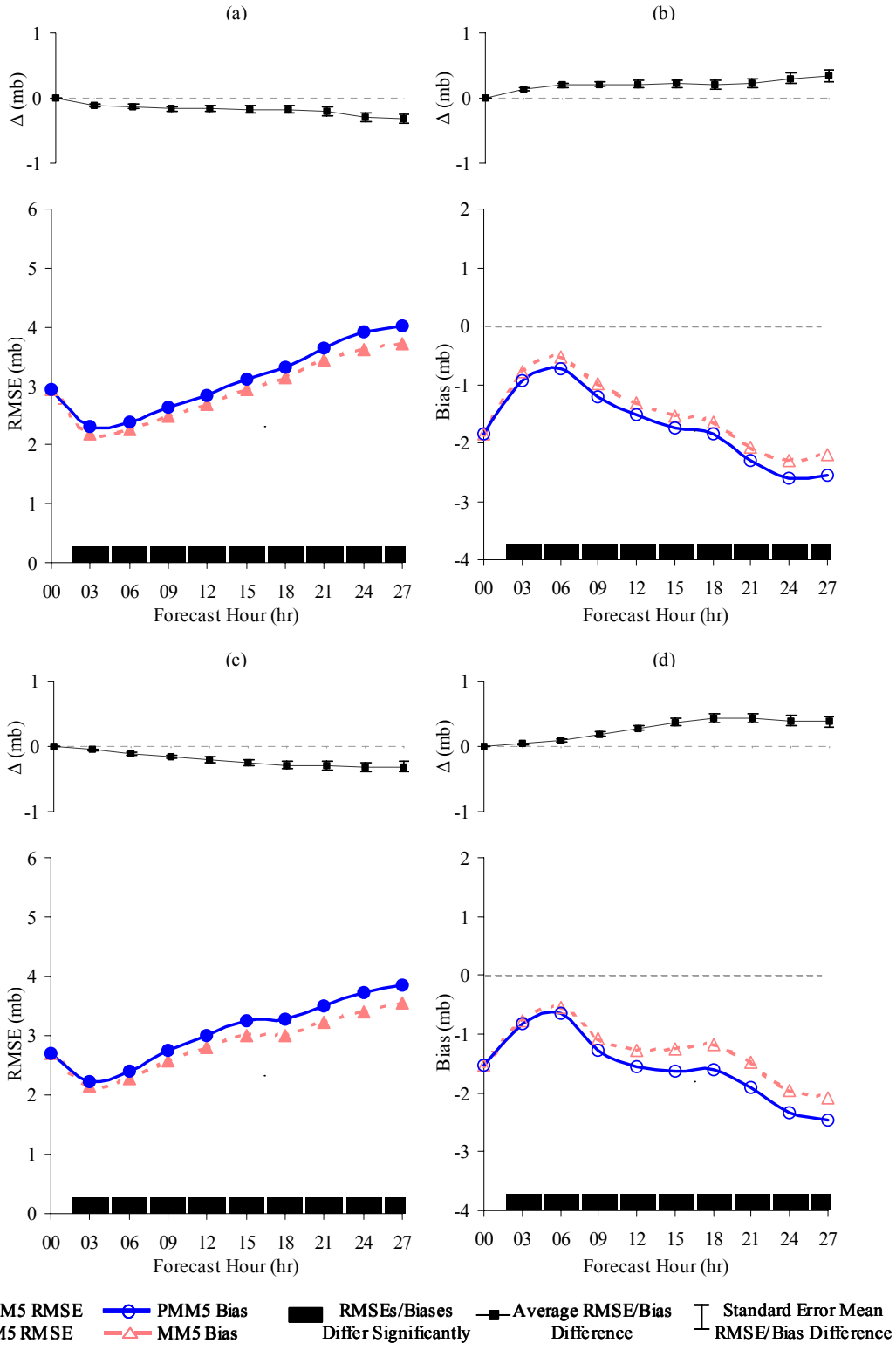

Figure 25. Mean Sea Level Pressure Verification Results. (a) & (b) 21 UTC initialization, same as Figure 17; (c) & (d) 09 UTC initialization, same as Figure 17.

runs separately. The model errors gradually increase throughout the forecast integration. The differences between the models increase slightly as well. While the significance tests show that there is a statistical difference between the RMSEs and biases of the two models, the magnitude of the differences is small. The average RMSE difference is 0.19 mb and the average bias difference is 0.23 mb. The pressure error comparison trends are similar to the temperature trends. The PMM5 RMSE is always greater than the MM5 RMSE, but the PMM5 produced a slightly more negative pressure bias than the MM5. These error differences are immeasurably small. There is no apparent diurnal trend in the pressure verification results.

4.4.1. By-Station MSL Pressure Analysis. Figure 26 is a representative depiction of the station MSL pressure RMSEs over all the forecast periods. The PMM5 RMSE of nearly all stations is greater than the MM5 RMSE. This relationship is in contrast to the very distinct regional differences found in the similar temperature comparison. The Interior region contains the stations with greatest contribution to overall error as well as differences

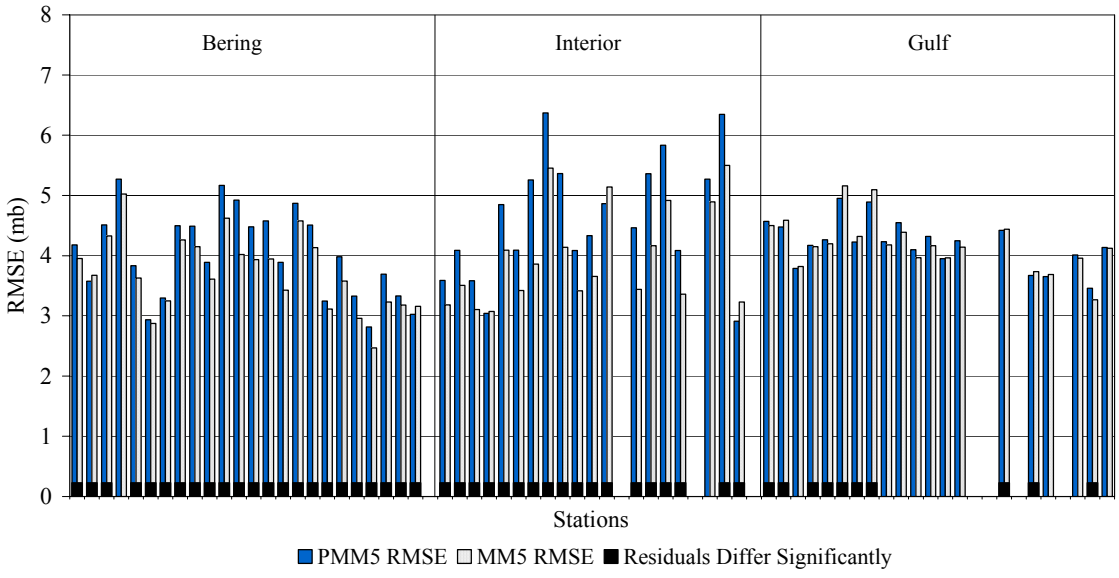

Figure 26. By-Station Surface MSL Pressure RMSE. 21 UTC 24 hour forecast

in error. The RMSE difference between the models at most stations was less than 1 mb. The significance tests failed to conclude that the models were statistically different for half of the stations in the Gulf Region.

Figure 27 shows a representative distribution of the station MSL pressure biases over all the forecast periods. Most stations in the Bering and Interior showed PMM5 biases exceeding MM5 biases, but the Gulf Region produced lower PMM5 biases compared to MM5 biases in the Gulf, which were similar to the temperature bias comparison. The average differences between the regional biases are not as distinct as the temperature bias differences between regions. The following section provides a summary of these regional comparisons of PMM5 results.

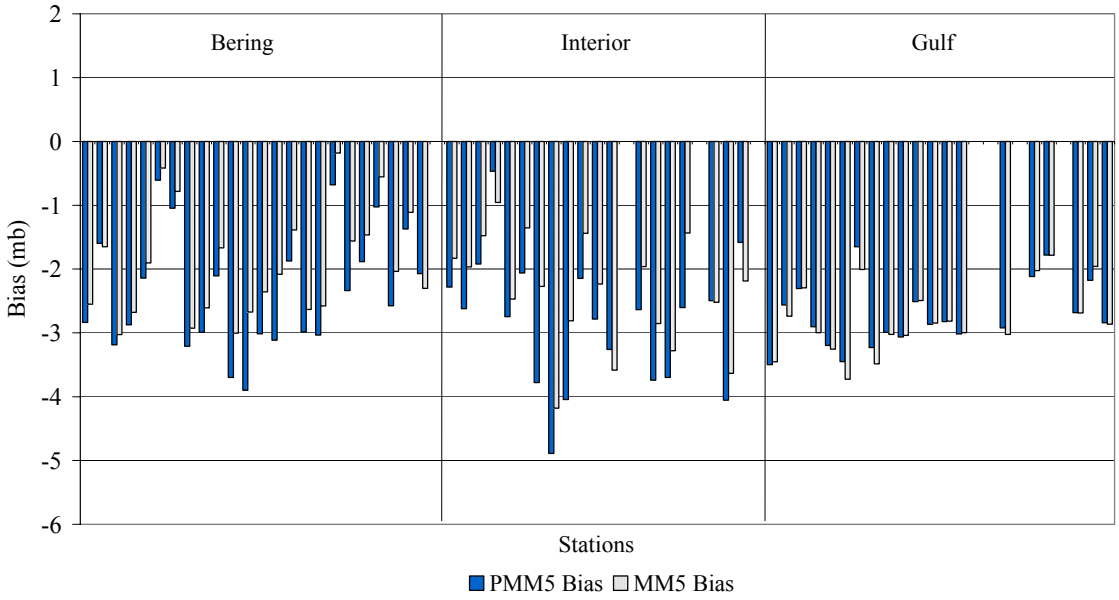

Figure 27. By-Station Surface MSL Pressure Bias. 21 UTC 24 hour forecast.

4.4.2. Regional MSL Pressure Analysis. Figure 28 summarizes the RMSE and bias differences between regions of the PMM5, which summarize the examples of the PMM5 RMSEs and biases shown in Figures 27 and 28. The MM5 regional comparisons

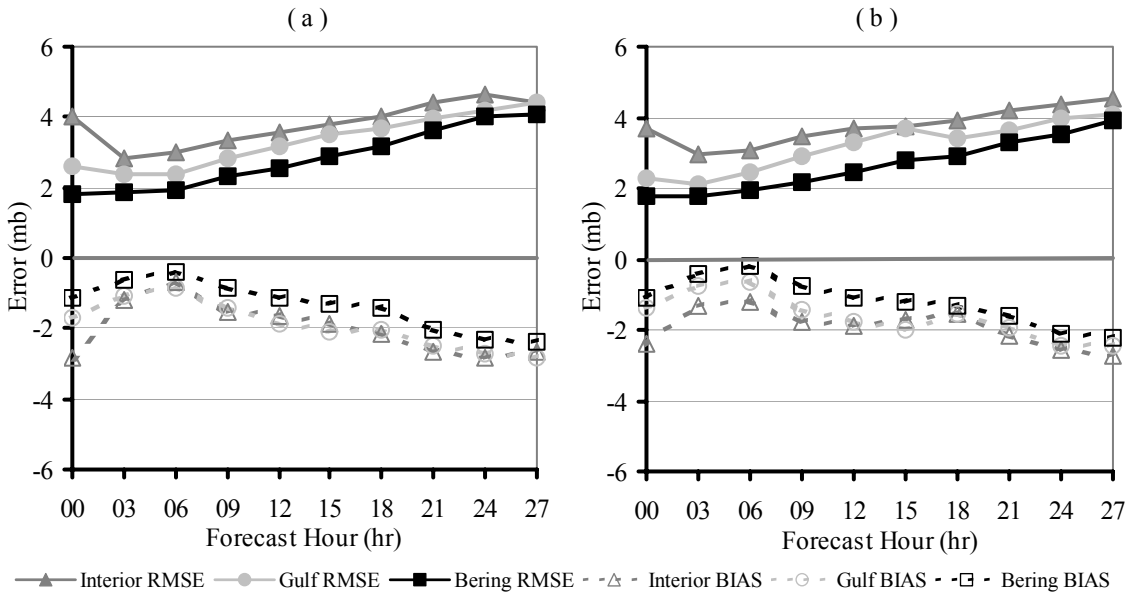

Figure 28. Regional PMM5 MSL Pressure RMSE and Bias Comparison. (a) 21 UTC initialization averages, (b) 09 UTC initialization averages.

contain identical relationships, which are consistent throughout all forecasts. The magnitude of all the error differences is not as significant as the regional temperature error differences. The Bering Region produced the least RMSE and least bias for all forecasts, where the Interior produced the greatest errors. This relationship is consistent with the regional temperature results. The thermodynamic link between temperature and pressure can be attributed to the agreement of this Bering-least-error/Interior-most-error relationship.

The regional differences in mean sea level pressure for the 21 UTC initialization runs are presented in Figure 29. The 09 UTC runs produced very similar results. The regional relationship between pressure differences remains consistent throughout the entire forecast duration. The higher Interior pressure bias errors of the PMM5 are also consistent with the lower temperature bias in this region. The greater pressure RMSEs of the PMM5 in correspond with the greater PMM5 temperature RMSEs in Figure 23.

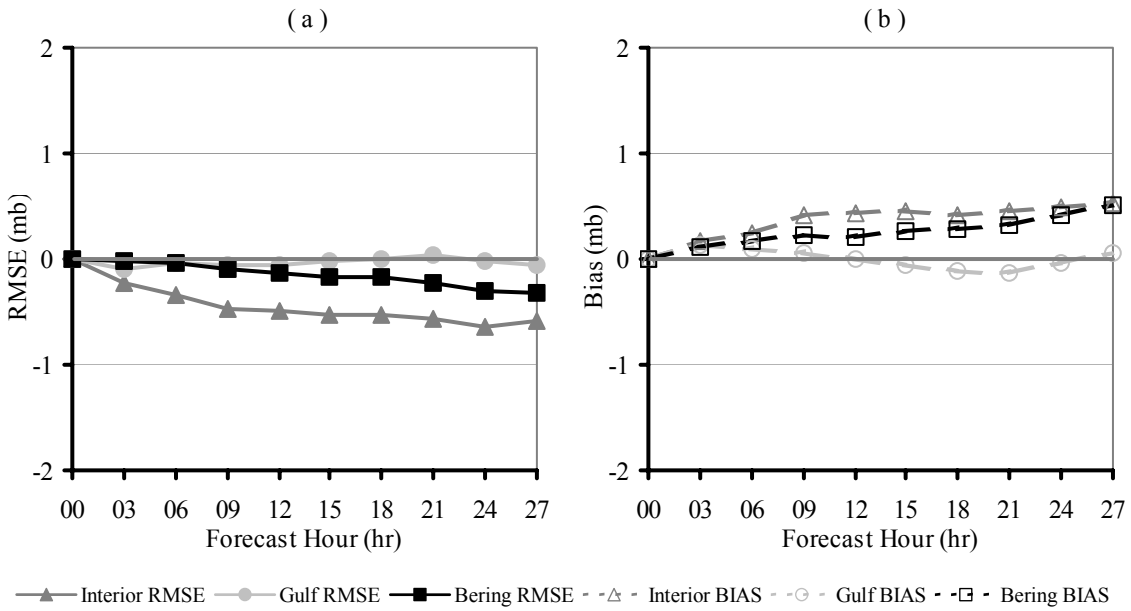

Figure 29. Regional MSL Pressure Model Error Differences (MM5-PMM5). (a) 21 UTC initialization MSL pressure RMSE, (b) 21 UTC initialization MSL pressure bias.

A station-specific analysis shows slight trends, but not as significant as was found for surface temperature. Figure 30 is a plot of all MSL pressure observations and 21 UTC 24-hour forecast values for Eielson (a) and Elmendorf (b) AFBs. The colder synoptic cases in November and December show a tendency of both models to under-forecast the MSL pressure at both locations. This is consistent with the warm biases present in the same forecasts. The models resolved most events very closely on this synoptic temporal scale.

4.5. Surface Wind Verification Results

RMSVE is the primary verification statistic used to compare the PMM5 with the MM5. RMSVE is described previously in section 3.5.2. The values of RMSVE are in units of speed, but do not necessarily correspond to speed errors exclusively. A perfect wind

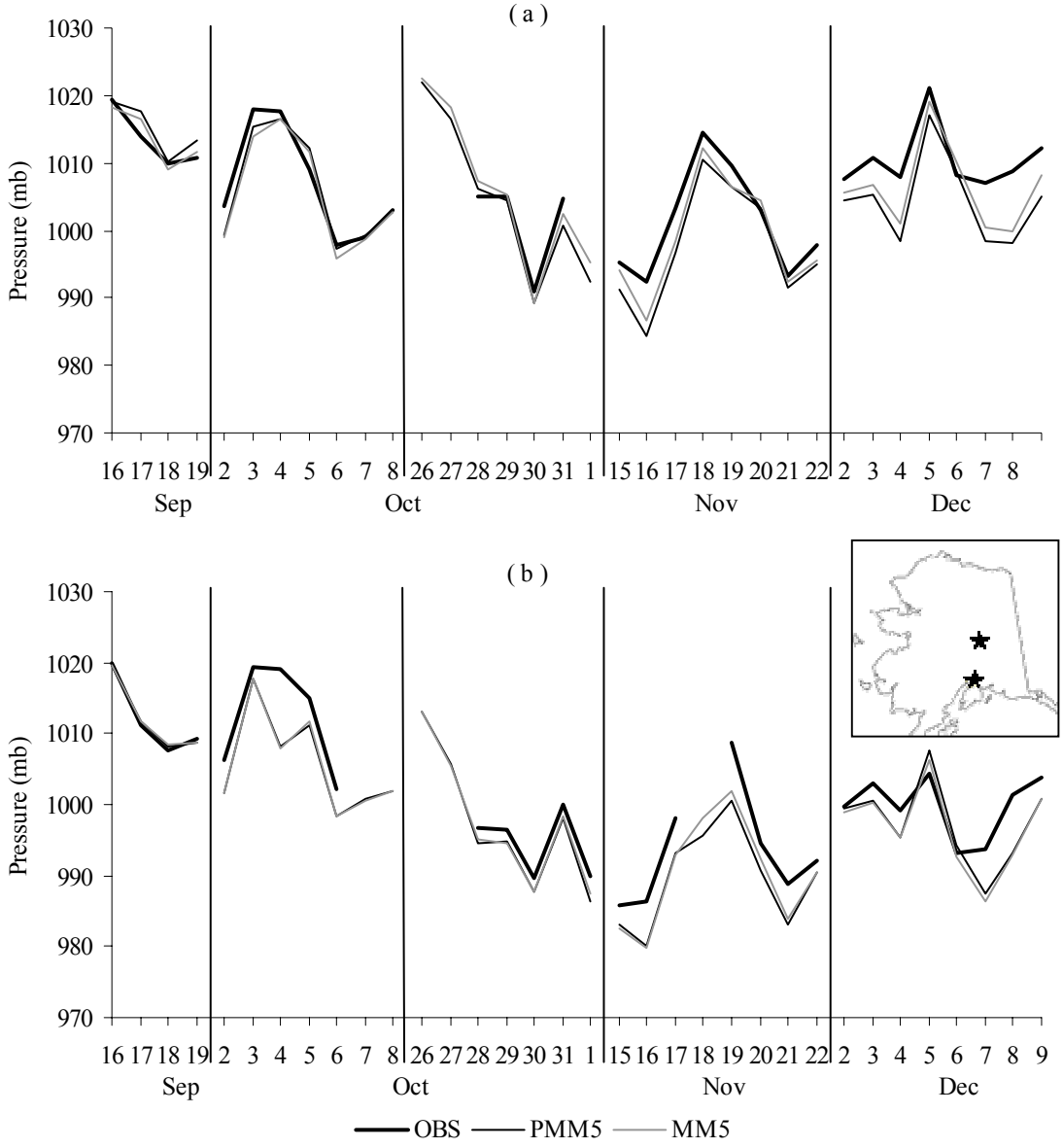

Figure 30. MSL Pressure Observation and Model Trends. 21 UTC 24-hour forecasts and observations for (a) Eielson AFB (northern star), and (b) Elmendorf AFB (southern star) by valid time. Vertical lines denote temporal breaks in forecasts.

speed forecast with a gross error in direction would result in a high value of RMSVE by the nature of the calculation following equation 7.

Figure 31 shows the average RMSVEs of all forecasts by forecast hour for the 21 and 09 UTC initializations. The variability in the wind error was on the order of several meters per second. The differences between the models were several orders of magnitude smaller

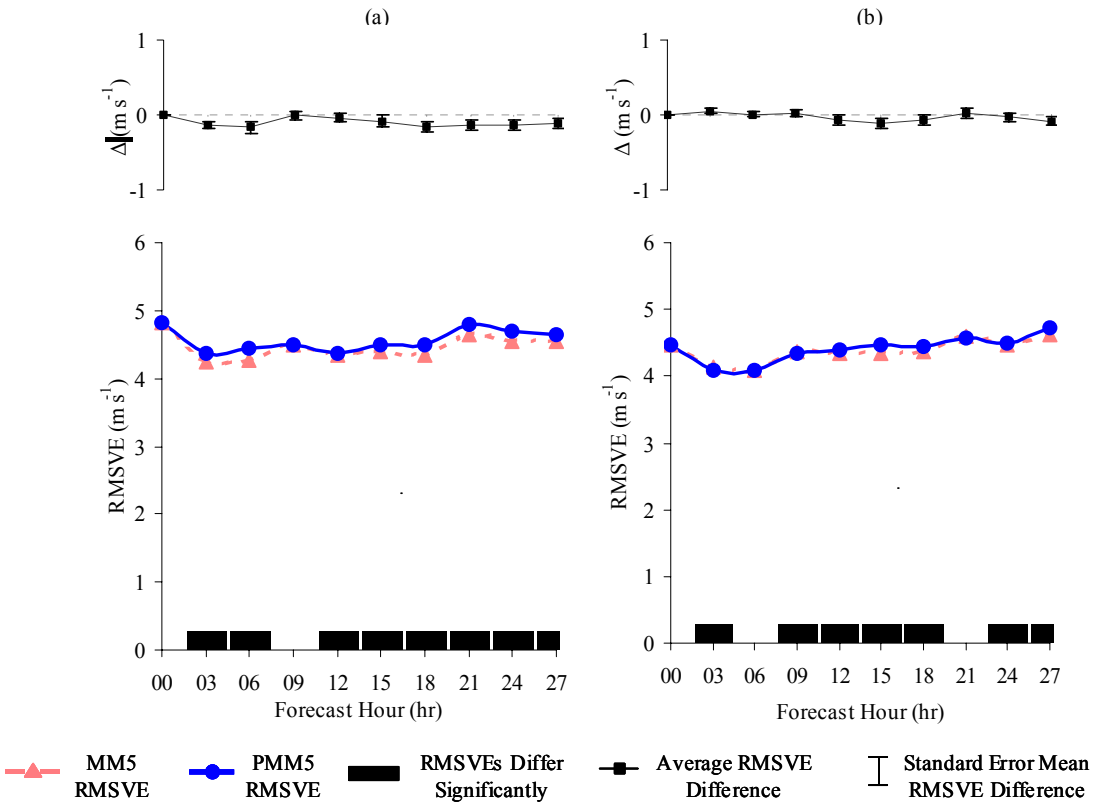

Figure 31. Surface Wind Verification Results. (a) 21 UTC initialization. (b) 09 UTC initialization

than the actual error. The average wind speed measurement accuracy of ±1 m s^{-1} and average wind direction measurement accuracy of ±5º constitute a comparable RMVSE accuracy of > 1 m s^{-1}, which is two orders of magnitude greater than the model RMSVE differences. The conclusion that the model average RMSVEs are identical is based on the very small model RMSVE differences (Δ) compared to measurable tolerances.

4.5.1. By-Station Surface RMSVE Analysis. The breakdown of the RMSVE by-station generates more insight than the domain-wide averages. Figure 32 is a representative distribution of the surface wind RMSVE values. The most apparent feature is the pronounced error of the Gulf stations exceeding nearly every station in the other two regions. There is no discernable difference between the models in any region as evident by the absence of any paired *t*-test null hypothesis rejections. This provides evidence that the

dynamic solutions of the two models are in very good agreement. This can be explained by the fact that the primary differences between the models are thermodynamic.

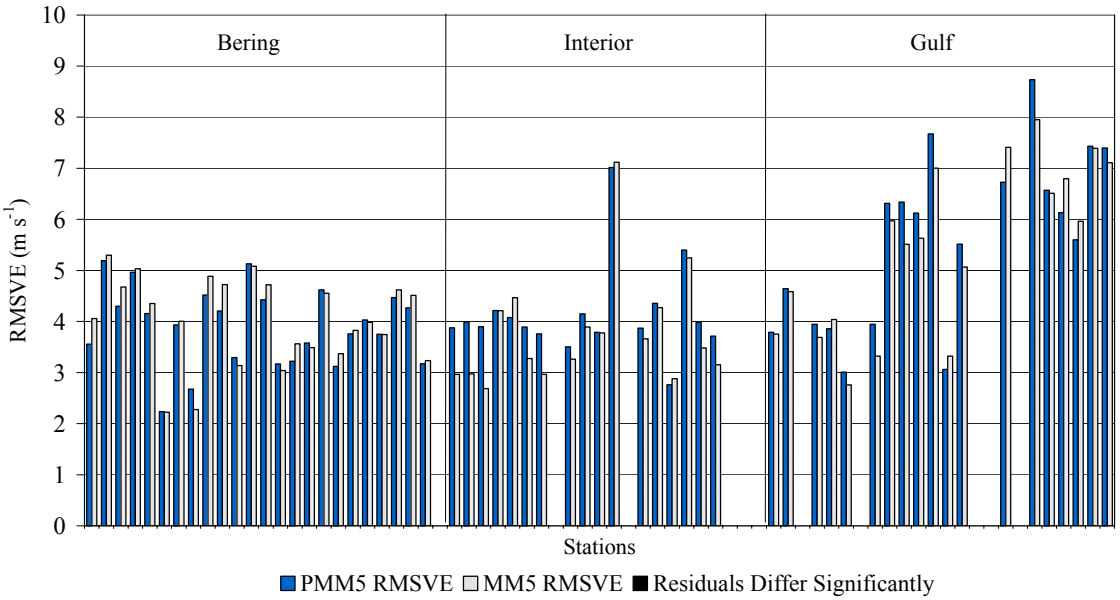

Figure 32. By-Station Surface Wind RMSVE. 09 UTC 21 hour forecast.

4.5.2. Regional Surface Wind Analysis. Figure 33 shows the pronounced difference in error between the Gulf and other regions. The significantly greater error in the

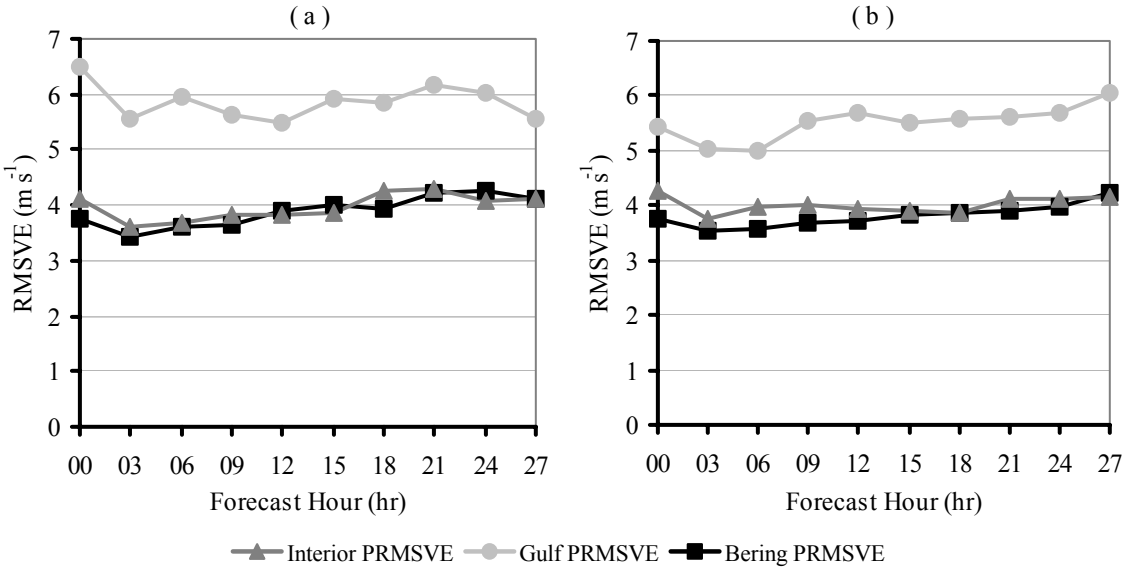

Figure 33. Regional PMM5 RMSVE Comparison. (a) 21 UTC initialization averages, (b) 09 UTC initialization averages.

Gulf could be attributed to the gross land/sea terrain errors. The Bering region contains coastline that is more gently sloped than the Gulf region. The average observed wind speed in the Gulf region was 3.21 m s^{-1}, compared to the Bering average wind speed of 4.45 m s^{-1}. This relationship would contradict the idea that the models would produce the greatest error in the windiest region. It is possible that the surface wind in the Gulf region had a greater directional variability than the Bering, leading to this error relationship.

The regional surface wind error differences between the PMM5 and MM5 is shown in Figure 34. The greater MM5 error exceeded the error of the PMM5 in the Gulf and Interior Regions. These differences are relatively small (~ 0.5 m s^{-1}) compared to the measurement accuracy. There was essentially no difference found in the Bering region.

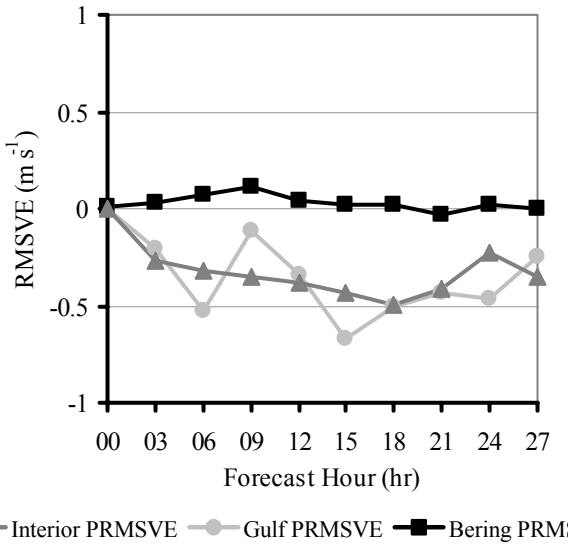

Figure 34. Regional Surface Wind Model Error Differences (MM5-PMM5) for 21 UTC runs.

The surface verification statistics show the greatest discrepancy between the models to be found in the temperature parameter. The differences in model error between the PMM5 and MM5 in pressure and wind parameters do not appear to be substantial. The preceding

sections have only verified a single layer of the atmosphere. The following sections will perform similar error comparisons for the entire three-dimensional volume of the domain.

4.6. Upper-Air Verification Results

The upper-air verification statistics were computed from only seven observation sites, in contrast to the 71 surface observation sites. This small number of verification sites contains every upper-air reporting location within the domain. The seven verification points are assumed to be representative of the entire grid (1725 km x 1455 km), an inescapable assertion with the sparse data population of Alaska.

Temperature, geopotential height, and relative humidity parameters are verified for comparison. The upper-air observations are taken every 12 hours, compared to the three hourly surface observation frequency used in the surface verification. The 27-hour simulation durations covered three upper-air reporting times at the 3, 15, and 27-hour forecasts. Every RAOB ended at or below 100 mb; therefore no verification was accomplished for the top two sigma levels above 100 mb.

The paired *t*-tests are conducted for each sigma level where the model data is verified against the interpolated RAOB. The significance tests determine the statistical bearing of the difference between the models' verification errors, RMSE and bias. The upper-air significance tests were conducted at the 95% confidence level with the same hypothesis, H_o: $\Delta=0$, as the surface tests described in section 3.5.2. The significance test results warrant additional interrogation. Figure 35 (a) is an example of the vertical temperature RMSE difference results. Figure 35 (a) shows an example of how the differences between the models are very close to zero, yet the paired *t*-tests declares the values as 'different'. A

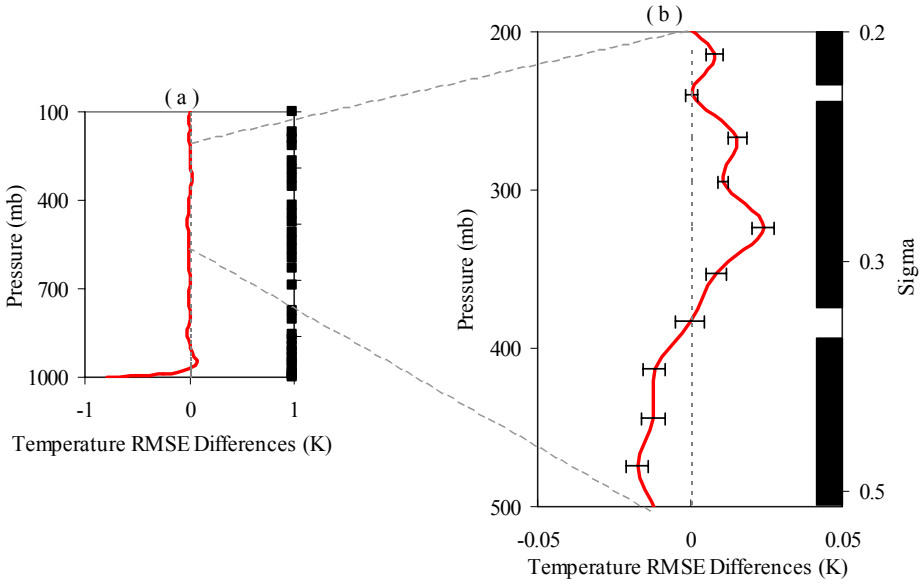

Figure 35. Significance Test Result Explanation. Differences (MM5-PMM5) in upper-air temperature RMSE for the 09 UTC initialization 15-hr forecast. The black bar denotes sigma levels of significant difference at the 95% confidence level. (a) The entire vertical column, (b) A zoomed in section of (a) with standard error mean bars.

zoomed in view of a portion of the region, Figure 35 (b), with the standard error mean bars provides some explanation. The tests on the sigma levels, where the standard error mean crosses zero fail to reject the null hypothesis, H_o: $\Delta=0$, were consistent with the statistical theory. However the scale on which this test is valid is one order of magnitude lower than the observational tolerance (±0.2 K) of the measuring equipment (Vaisala, 2002).

4.6.1. Upper-Air Temperature Verification Results. The domain temperature RMSE and bias are calculated in the same manner as the surface temperature statistics described in section 3.5.2. The same difference, Δ=MM5-PMM5, is also consistent with the surface verification comparisons. The vertical RMSE traces for the PMM5 and MM5 were similar enough to exclude the actual RMSE traces and focus on the differences. Figure 36 represents the temperature RMSE differences (Δ) between the models on sigma levels. The charts show areas in the vertical where the PMM5 produced greater errors than the MM5 when the trace

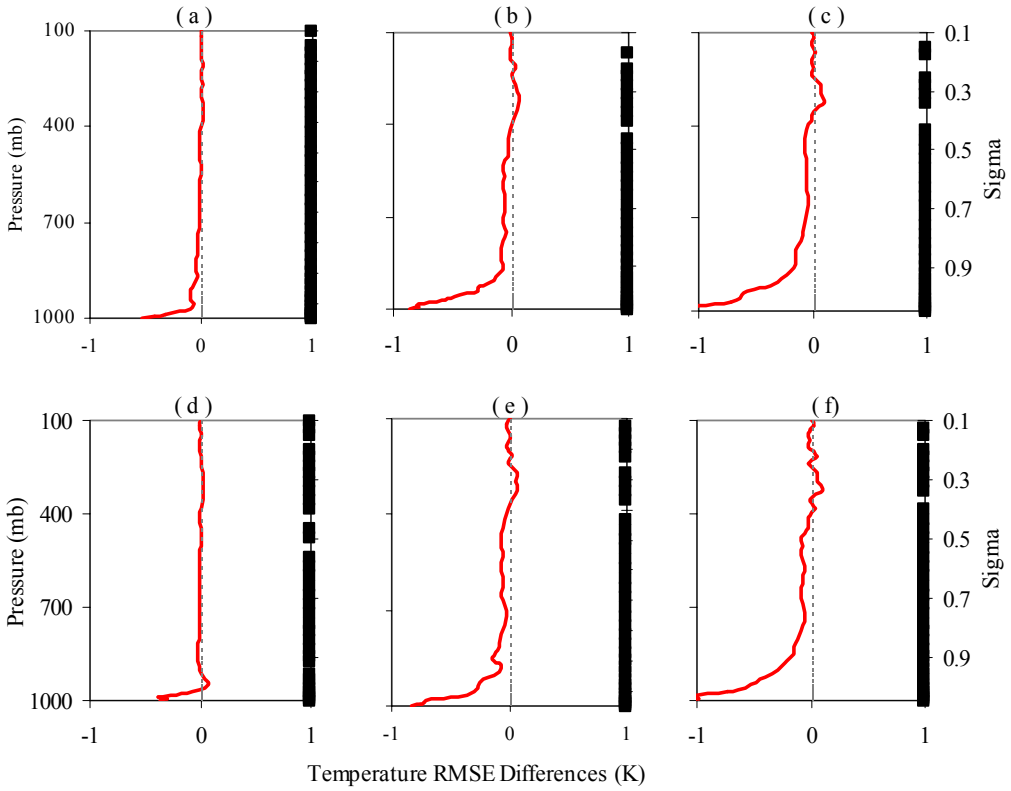

Figure 36. Average Differences (MM5-PMM5) in Upper-Air Temperature RMSE. 21 UTC initialization runs (a) 3-hr, (b) 15-hr, (c) 27-hr and 09 UTC initialization runs (d) 3-hr, (e) 15-hr, (f) 27-hr. The black bar denotes sigma levels of significant difference at the 95% confidence level.

is in the negative region. Conversely, a positive difference depicts a greater error produced by the MM5. It is important to remain cognizant of the difference scale when interpreting these vertical difference charts.

While the paired *t*-tests define the differences at nearly every sigma level as statistically significant, the differences are negligible in magnitude except for the near-surface atmosphere. The lowest sigma levels produced model differences that are consistent with the surface differences. The PMM5 temperature RMSEs are greater than MM5 temperature RMSEs in the lowest 100 mb.

The average bias differences can filter out information by averaging positive and negative values. The actual bias profiles of the two models are plotted for this reason rather

than bias differences. Figure 37 displays the temperature bias profiles of the PMM5 and MM5. Both models are in close agreement throughout the entire vertical column. The MM5 biases are lower (closer to zero) than the PMM5 biases for the 21 UTC runs in the lowest 100 mb of the atmosphere. This lowest 100mb comparison is reversed in the 09 UTC runs. The degree of difference is much less than 1 K and deemed insignificant, even though the two bias trends are statistically different at nearly every level by the paired *t*-test. The most notable feature is the significant warm biases both models posses in the upper atmosphere. These trends are consistent with a discrepancy in the location of the tropopause. The tropopause location is critical given the sharp thermodynamic contrast across the layer. This feature is evident in the geopotential biases seen in the following section.

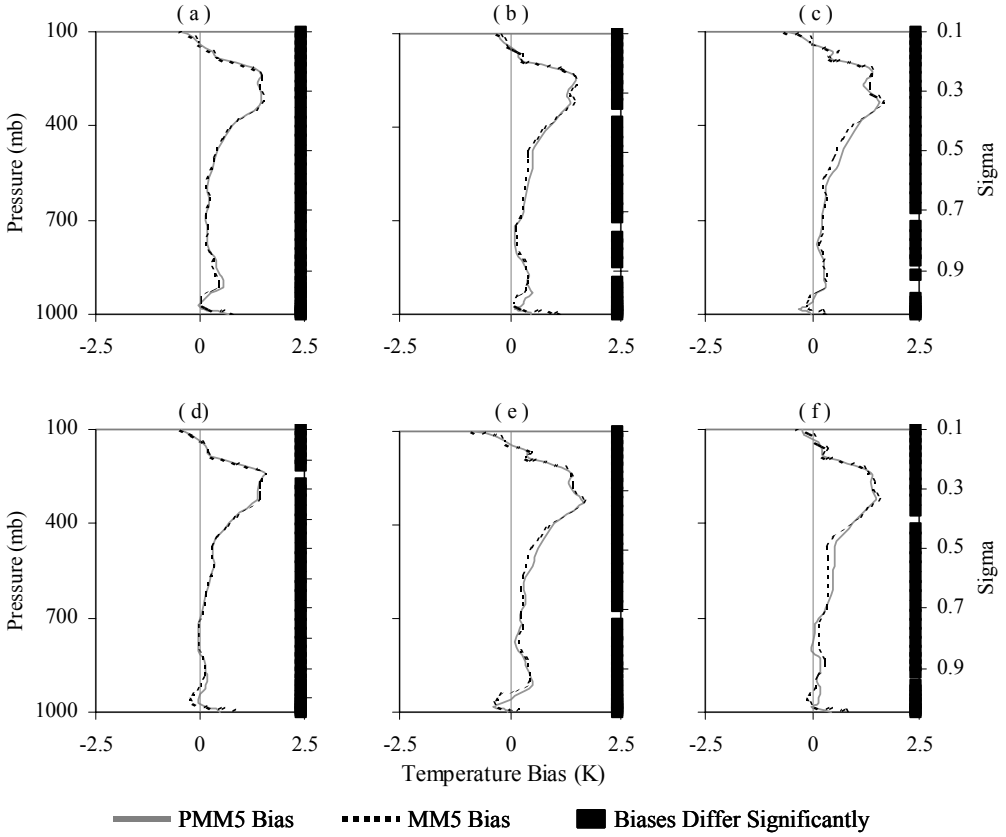

Figure 37. Average Upper-Air Temperature Bias of PMM5 and MM5. 21 UTC initialization (a) 3-hr, (b) 15-hr, (c) 27-hr and 09 UTC initialization (d) 3-hr, (e) 15-hr, (f) 27-hr. The black bar denotes sigma levels of significant difference at the 95% confidence level.

4.6.2. Upper-Air Geopotential Height Verification Results. The geopotential height verification differences closely resemble the temperature findings as a result of the thermodynamic dependence of the geopotential height calculation. Figure 38 illustrates the small differences in geopotential height RMSE between the models. The largest differences were above 400 mb, the same region where the maximum temperature bias was found. The PMM5 appears to handle the tropopause slightly better than the MM5, based on the greater MM5 error (positive Δ) above 400 mb. The geopotential height biases in Figure 39 provide more insight. The RMSE and bias differences are less than five geopotential meters (gpm) at every level, which is well within the measurement tolerance.

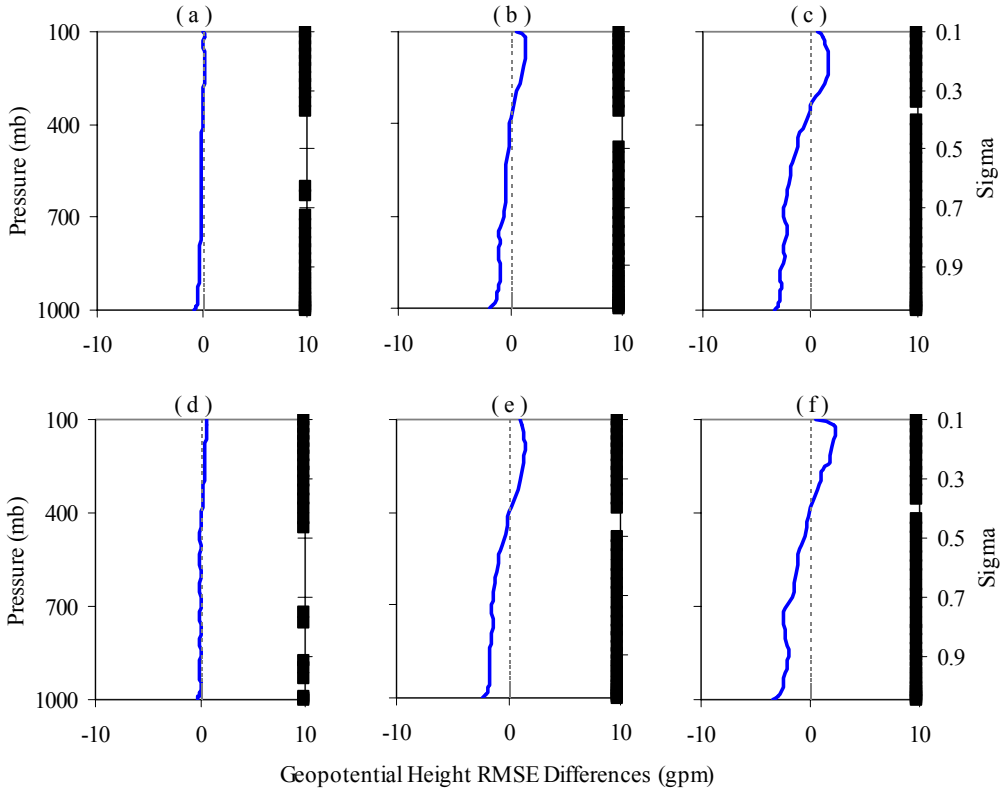

Figure 38. Average Differences (MM5-PMM5) in Upper-Air Geopotential Height RMSE. Same as Figure 36.

The plots of average biases in the vertical profiles are found in Figure 39. The relatively minute differences between the models are apparent. The PMM5 and MM5

possess similar biases throughout the entire vertical column for all forecast times. The pronounced over-predicted geopotential height above 400 mb is likely a result of the inaccurate forecast placement of the tropopause. These strong biases vertically correspond to the warm biases found in the temperature fields. This is meteorologically consistent, as higher heights would result from warmer temperature. Personal conference with Dr. Bromwich at the BPRC alluded to the theory that there is still a gravity wave corruption near the top of the atmosphere that might cause these results. A suggested solution in previous work (Bromwich et al., 2001b) was to set the model top above 100 mb to alleviate this bias. The model top for this project was 50 mb, but the problem persisted.

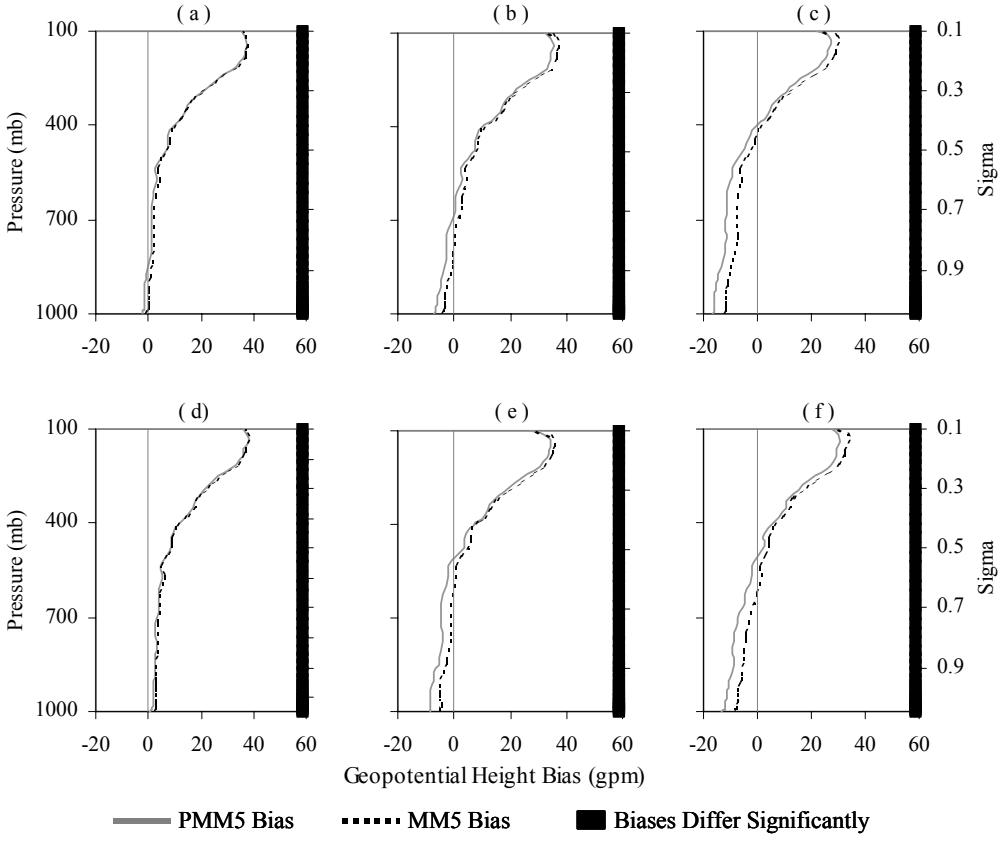

Figure 39. Average Upper-Air Geopotential Height Bias of PMM5 and MM5. Same as Figure 37.

4.6.3. Upper-Air Relative Humidity Verification Results. The measurement of moisture presents comparison challenge that were not a factor with the previously verified parameters. The measurement error of moisture is proportional to the magnitude of the moisture present. For this reason, normalization to the observed state was necessary. Relative humidity (RH) was calculated for RAOBs and model output. The RH residuals were normalized to the observed value by equation 11,

$$\text{residual} = \frac{(\text{model} - \text{observation})}{\text{observation}} \times 100\% . \tag{11}$$

This normalization allows a comparison to made between the differences on varying orders of magnitude. The normalized RH RMSE and bias values describe a relationship based on the available moisture opposed to the strict model-observed difference and are in units of percentage of the observed quantity.

The PMM5 and MM5 normalized RH RMSE differences are plotted in Figure 40. The models are in close agreement above 700mb. The low-levels and a 700mb spike show the only measurable differences. The PMM5 consistently produced greater errors in the low levels (< 700 mb) than the MM5. An analysis of the normalized RH biases in Figure 41 shows that the PMM5 is slightly over-predicting the low-level moisture by 10% of observed RH over the MM5. There is an apparent decrease in bias from 700-900 mb in all forecast times with a marked moist bias in the mid-levels (500-700 mb). The PMM5 generated greater moisture error in the lowest 100 mb over the MM5. There is a consistent layer between 800-900 mb where the MM5 generated greater error than the PMM5. The over/under-prediction of these moisture errors is observed in Figure 41. The PMM5 and MM5 moisture biases display similar trends

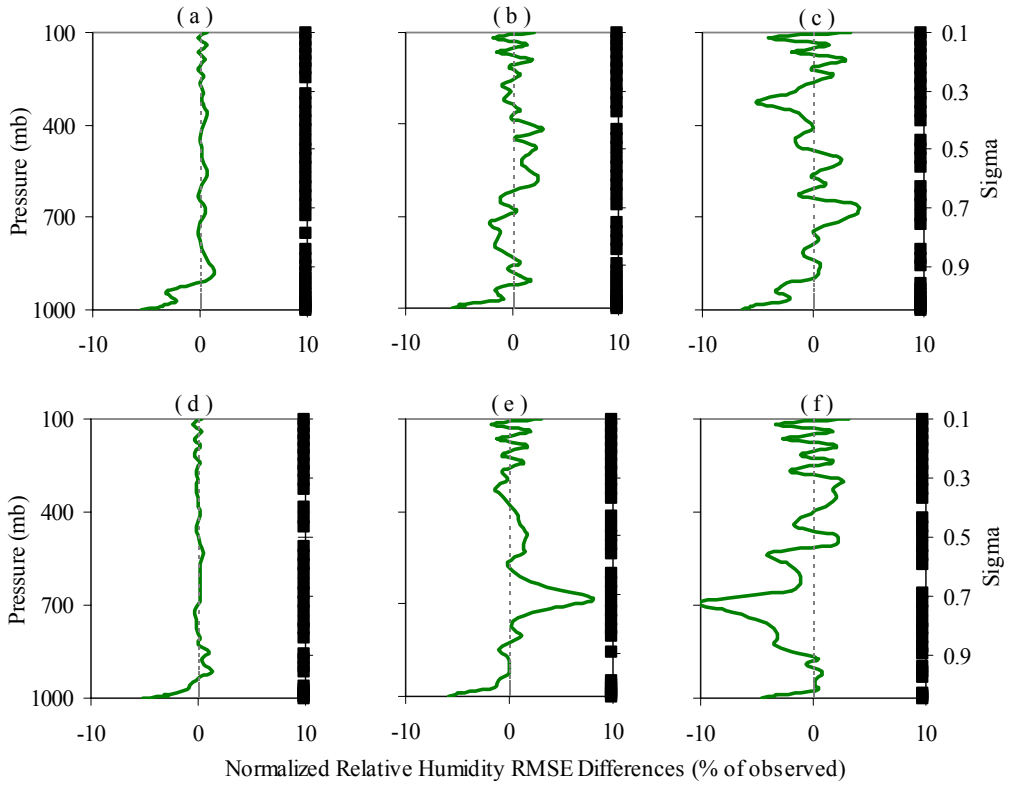

Figure 40. Average Differences (MM5-PMM5) in Upper-Air Relative Humidity RMSE. 21 UTC initialization (a) 3-hr, (b) 15-hr, (c) 27-hr and 09 UTC initialization runs (d) 3-hr, (e) 15-hr, (f) 27-hr. The black bar denotes sigma levels of significant difference at the 95% confidence level.

for the 09UTC and 21 UTC initialization runs. The PMM5 3-hr forecast has a low-level moist bias where the MM5 is neutral. This implies that the PMM5 may be more sensitive to the initial spin-up of moisture in the model, which is carried through the simulation.

The intended goal of the PMM5 moisture modifications was to diminish the excessive ice cloud produced by the MM5. The extreme temperatures found in the December forecasts may have affected these low-level moisture calculations. It is possible that the Meyers equation (equation 4) used in the PMM5 for ice nuclei concentration may have induced the moisture over-prediction in the low levels during these extreme low-temperature situations.

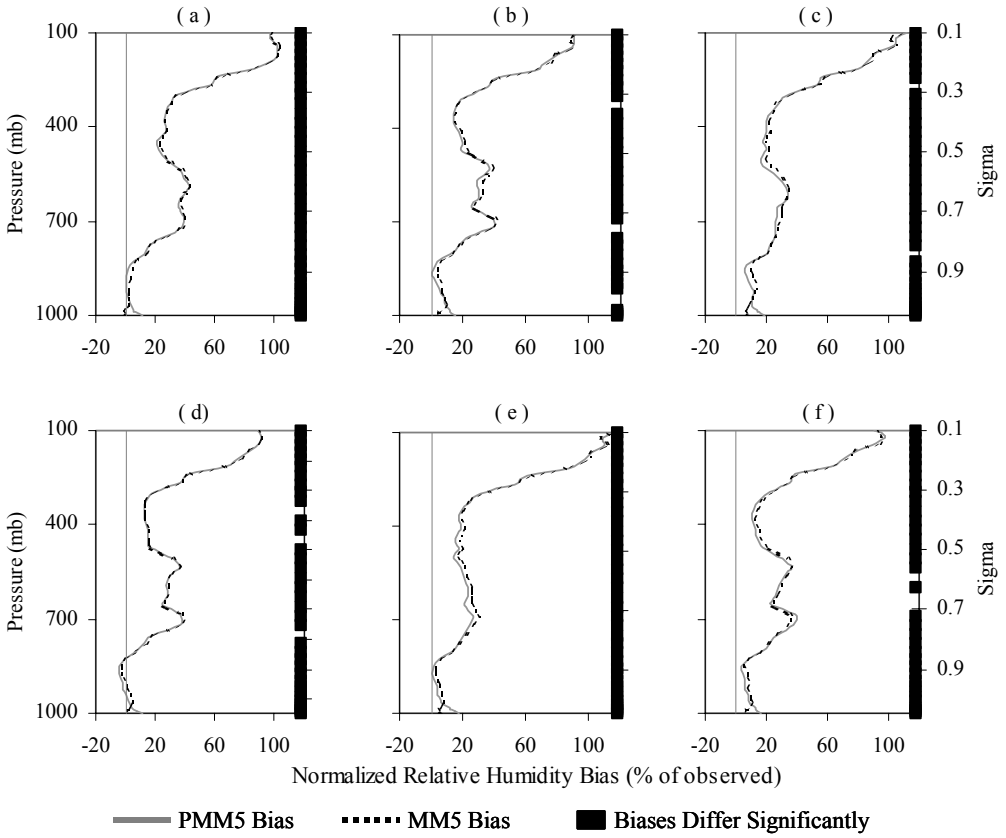

Figure 41. Average Upper-Air Relative Humidity Bias of PMM5 and MM5. Same as Figure 40.

V. Conclusions and Recommendations

5.1. Conclusions

This research explored the comparison of the Polar MM5 to a replicated version of the MM5 run operationally at the Air Force Weather Agency (AFWA). This project presents the first forecasts of this modified weather model over Alaska. Several meteorological parameters were verified from 67 forecasts. The simulated scenarios ranged over a four-month period of non-consecutive weeks to ensure that a maximum variety of weather regimes were modeled. These verification results can be used for further understanding and comparison of the Polar MM5 performance over other regions of applicability such as Greenland and Antarctica.

The original objectives achieved included compiling, executing, and verifying the PMM5. These tasks were accomplished to meet the objectives of comparing the PMM5 verification results to the MM5 and assessing any differences. The main focus of this research was to assess the utility of replacing the operational AFWA MM5 with the PMM5 over the Alaskan region.

The tremendous collection of comparisons analyzed in this research provides evidence of significant difference between the PMM5 and MM5 in surface temperature bias and low-level moisture. There were also sufficient results to show the spatial distribution of the error that both models shared in three climatological regions. The PMM5 produces greater surface and low-level temperature RMSEs than the MM5, while producing smaller low-level temperature biases. The *variability* in PMM5 error over the MM5 would produce

this relationship. The exclusion of a few stations producing gross errors might bring the PMM5 RMSEs down below the MM5 RMSEs.

While the PMM5 may be producing a more physically realistic forecast when analyzing the entire domain, the utility for the Air Force forecaster is the pinpoint station accuracy. The results discovered in this research do not appreciably support using the PMM5 as an operational replacement to the MM5 over Alaska.

5.2. Recommendations

While this project interpreted many verification statistics between the PMM5 and MM5 over Alaska, the comparison was less than exhaustive. This research was very limited on time and resources. A more thorough assessment of model comparison should ideally cover all seasons and extend the simulation duration beyond a 27-hour forecast. The interrogation of horizontal features would be the most beneficial comparison beyond the results presented here. One model may be resolving features more accurately than the other, but slight placement errors could yield worse pinpoint errors. A grid-to-grid comparison can be used to generate an objective analysis between the models, but the non-uniform distribution of observation locations adds complications to this technique.

A focused interrogation of the specific impact of the polar modifications over Alaska may provide some scientific rationale defining the results presented. Searching for clues to the regional discrepancies of the models may come from analyzing correlations between the radiation, moisture, and temperature parameters.. This could lead to further modifications specialized for the Polar Regions.

The field of numerical weather prediction will continue to evolve based on results of test-and-compare projects. The specialization of a mid-latitude forecasting tool to a high latitude region is desirable for such regions were DoD possesses valuable assets and where extreme atmospheric conditions routinely threaten life and property. The individual forecaster issuing the terminal aerodrome forecast, who serves as the interface between science and operations, will reap a great benefit of any improvement in atmospheric modeling over Alaska.

Bibliography

Arakawa, A., and V.R. Lamb, 1977: Computational design of the basic dynamical process of the UCLA general circulation model. *Methods in Computational Physics*, **17**, 173-265.

Bresch, J., NCAR, Personal Correspondence. 15-25 September 2001.

Bromwich, D.H., Polar Meteorology Group, Byrd Polar Research Center, The Ohio State University, OH. Personal Interview. 10 August 2001a.

-----, J.J. Cassano, and T. Klein, G. Heinemann, K.M. Hines, K. Steffen, J.E. Box, 2001b: Mesoscale modeling of katabatic winds over Greenland with the Polar MM5. *Mon. Wea. Rev.*, **129**, 2290-2309.

Bougeault, P., 1983: A non-reflective upper boundary condition for limited-height hydrostatic models. *Mon. Wea. Rev*., **111**, 420-429.

Department of the Air Force. *Wind Measuring Set, AN/GMQ-20 (V).* T.O. 31M5-2GMQ20-2. McClellan AFB, CA: SM-ALC/LICDA, 15 February 1994.

-----. *Digital Altimeter-Barometer, ML-658/GM.* T.O. 31M1-2GM-61. McClellan AFB, CA: SM-ALC/LICDA, 15 April 1997.

-----. *Ambient Temperature and Dewpoint Measuring Set, AN/FMQ-8*. T.O. 31M1-2FMQ8-1. McClellan AFB, CA: SM-ALC/LICDA, 16 August 1998.

Dudhia, J, D. Gill, Y. Guo, K. Manning, W. Wang, 2001: PSU/NCAR Mesoscale Modeling System, Tutorial Class Notes and User's Guide: MM5 Modeling System Version 3. [Available on-line from http://www.mmm.ucar.edu/mm5/doc.html.]

Ebert, E.E., and J.A. Curry, 1992: A parameterization of ice cloud optical properties for climate models. *J. Geophys. Res*., **97**, 3831-3836.

Fletcher, N.H., 1962: *Physics of Rain Clouds*. Cambridge University Press, 386pp.

Grell, G.A., J. Dudhia, D.R. Stauffer, 1995: A description of the fifth-generation Penn State/NCAR mesoscale model (MM5). NCAR Tech. Note NCAR/TN-398+STR, 122pp.

Hack, J.J., B.A. Boville, B.P. Briegleb, J.T. Kiehl, P.J. Rasch, and D.L. Williamson, 1993: Description of NCAR community climate model (CCM2). NCAR Tech. Note NCAR/TN-382+STR, 108pp.

Hines, K.M., D.H. Bromwich, and Z. Liu, 1997a: Combined global climate model and Mesoscale model simulations of Antarctic climate, *Ann. Glaciol*., **25**, 282-286.

Hines, K.M., D.H. Bromwich, and R.I. Cullather, 1997b: Evaluating moist physics for Antarctic mesoscale simulations, *J. Geophys. Res.*, **102**, 13747-13760.

Houghton, H.G., 1985: *Physical Meteorology*. Cambridge Press, 442 pp.

Klemp, J.B. and D.R. Durran, 1983: An upper boundary condition permitting internal gravity wave radiation in numerical mesoscale models. *Mon. Wea. Rev*., **111**, 430-444.

Liou, K.N., 1974: On the radiative properties of cirrus in the window region and their influence on remote sensing of the atmosphere. *J. Atmos. Sci.*, **31**, 522-532.

List, R., 1984: *Smithsonian Meteorological Tables*. Smithsonian Institution Press, 527 pp.

Mannarano, D., "Automated Surface Observing System Users Guide." Product information, http://www.nws.noaa.gov/asos/index.html. March 1998.

Manning, K.W. and C.A. Davis, 1997: Verification and sensitivity experiments for the WISP94 MM5 forecasts. *Wea. Forecasting*, **12**, 719-735.

Meyers, M.P., P.J. DeMott, and W.R. Cotton, 1992: New primary ice-nucleation parameterizations in an explicit cloud model. *J. Appl. Meteor.*, **31**, 708-721.

National Snow and Ice Data Center, "Arctic Climatology and Meteorology Primer." Excerpt from training module. http://nsidc.org/arcticmet. 20 October 2001.

Reisner, J., R.M. Rasmussen, and R.T. Bruintjes, 1998: Explicit forecasting of supercooled liquid water in winter storms using the MM5 mesoscale system. *Quart. J. Roy. Meteor. Soc.*, **124**, 1071-1107.

Rogers, R.R. and M.K. Yau, 1991: *Introduction to Cloud Physics*. Pergamon Press, 293 pp.

Swanson, R., Air Force Weather Agency, NE, Personal Correspondence. 30 October 2001.

Tilley, J., University of Alaska Fairbanks, AK, Personal Correspondence. 10-20 August 2001.

Vaisala, "Technical Information on Radiosonde, model RS80" Product information. http://www.vaisala.com. 8 January 2002.

Vukicevic, T.T., and J. Paegle, 1989: The influence of one-way interacting lateral boundary conditions upon predictability of flow in bounded numerical models. *Mon. Wea. Rev*., **117**, 340-350.

Wallace, J.M., P.V. Hobbs, 1977: *Atmospheric Science, An Introductory Survey*. Academic Press, 467 pp.

Wilkes, D.S., 1995: *Statistical Methods in the Atmospheric Sciences*. Academic Press, 467 pp.

Yen, Y.C., 1981: *Review of thermal properties of snow, ice, and sea ice*. CRREL Rep. 81-10, 27pp.

Table A-1. Physical Parameters of Land-use Categories (provided with PMM5 code, NCAR, 2001)

Landuse Integer ID	Landuse Description	Albedo (%)		Mositure Available (%)		Emissivity (% at 9 mm)		Roughness Length (cm)		Thermal Inertia (cal cm^{-2} K^{-1} $s^{-½}$)	
		Winter	Summer	Winter	Summer	Winter	Summer	Winter	Summer	Winter	Summer
1	Urban and Built-Up Land	18	18	10	10	88	88	50	50	0.03	0.03
2	Dryland Cropland and Pasture	23	17	60	30	92	92	5	15	0.04	0.04
3	Irrigated Cropland and Pasture	23	18	50	50	92	92	5	15	0.04	0.04
4	Mixed Dryland/Irrigated Cropland	23	18	50	25	92	92	5	15	0.04	0.04
5	Cropland/Grassland Mosaic	23	18	40	25	92	92	5	14	0.04	0.04
6	Cropland/Woodland Mosaic	20	16	60	35	93	93	20	20	0.04	0.04
7	Grassland	23	19	30	15	92	92	10	12	0.04	0.03
8	Shrubland	25	22	20	10	88	88	10	10	0.04	0.03
9	Mixed Shrubland/Grassland	24	20	25	15	90	90	10	11	0.04	0.03
10	Savanna	20	20	15	15	92	92	15	15	0.03	0.03
11	Deciduous Broadleaf Forest	17	16	60	30	93	93	50	50	0.05	0.04
12	Deciduous Needleleaf Forest	15	14	60	30	93	94	50	50	0.05	0.04
13	Evergreen Broadleaf Forest	12	12	50	50	95	95	50	50	0.05	0.05
14	Evergreen Needleleaf Forest	12	12	60	30	95	95	50	50	0.05	0.04
15	Mixed Forest	14	13	60	30	94	94	50	50	0.06	0.04
16	Water Bodies	8	8	100	100	98	98	0.01	0.01	0.06	0.06
17	Herbaceous Wetland	14	14	75	60	95	95	20	20	0.06	0.06
18	Wooded Wetland	14	14	70	35	95	95	40	40	0.06	0.05
19	Barren or Sparsely Vegetated	25	25	5	2	85	85	10	10	0.02	0.02
20	Herbaceous Tundra	60	15	90	50	92	92	10	10	0.05	0.05
21	Wooded Tundra	50	15	90	50	93	93	30	30	0.05	0.05
22	Mixed Tundra	55	15	90	50	92	92	15	15	0.05	0.05
23	Bare Ground Tundra	70	25	95	2	95	85	5	10	0.05	0.02
24	Snow or Ice	70	55	95	95	95	95	5	5	0.05	0.05
25	Permanent ice	82	80	95	95	95	95	0.01	0.01	0.05	0.05
26	Sea ice	82	80	95	95	95	95	0.1	0.1	0.05	0.05

Appendix B. Interpolation Technique

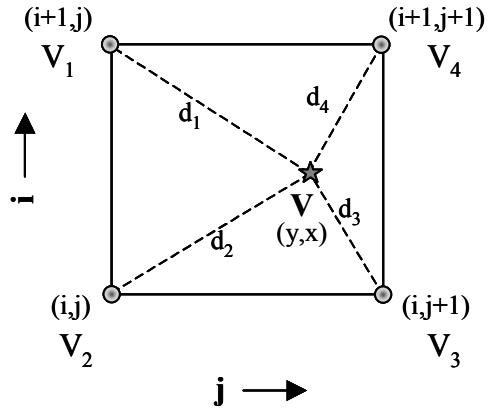

Figure B-1. Interpolation Description. The star represents the station location with the four surrounding grid points (circles). Grid coordinates are i and j (convention consistent with the MM5 grid). The variable value at each of the four points is labeled as V_1,V_2,V_3, and V_4 with the desired interpolated station variable value as **V**. The distance from the station location on the grid (y,x) to the four grid points is labeled as d_1, d_2, d_3, and d_4.

The inverse-weighted linear interpolation method is described in this appendix. Figure B-1 presents a graphical depiction of the process. The distances between the station and the four surrounding grid points are calculated using the Pythagorean theorem. The distance will be used to weight the variable values of each grid point. The coordinates of (y,x) represent the grid location of the station on the MM5 grid in fractions of grid points. The (y,x) values were provided by AFWA, but can be generated by RIP when plotting vertical profiles.

$$d_1 = \sqrt{[(i+1)-y]^2 + (x-j)^2} \tag{B-1}$$

$$d_2 = \sqrt{(y-i)^2 + (x-j)^2} \tag{B-2}$$

$$d_3 = \sqrt{(y-i)^2 + [(j+1)-x]^2} \tag{B-3}$$

$$d_4 = \sqrt{[(i+1)-y]^2 + [(j+1)-x]^2} \tag{B-4}$$

The four distances are summed,

$$D = \sum_{n=1}^{4} d_n \quad . \tag{B-5}$$

The ratio of each distance to the sum of the distances, D, is calculated,

$$ratio_n = \frac{d_n}{D} \quad . \tag{B-6}$$

The sum of the ratios is unity. The inverse-weighting is applied as unity minus the individual ratio,

$$weight_n = 1 - ratio_n \quad . \tag{B-7}$$

The weighting factors are applied to the individual variable values at the respective grid point. Finally the sum of the weighted values ($V_n \cdot weight_n$) is normalized by the sum of the weights.

$$V = \frac{\sum_{n=1}^{4} \left(V_n \cdot weight_n \right)}{\sum_{n=1}^{4} weight_n} \tag{B-8}$$

Vita

Captain William E. Courtemanche attended undergraduate school in Meteorology and Environmental Science at Lyndon State College of Vermont where he received a Bachelor of Science degree in 1995. He was commissioned through Detachment 865 AFROTC and entered the Air Force in August 1995. The Air Force fulfilled his life-long goal of working in the field of meteorology in Alaska, which subsequently led to this research project.

His first assignment was at Eielson AFB outside Fairbanks, Alaska as an operational meteorologist. While stationed at Eielson, he redesigned forecasting aides, conducted case studies, and was identified as an outstanding technical and operational performer in a Standardization and Evaluation inspection. He concurrently attended graduate classes at the University of Alaska Fairbanks in the Atmospheric Science Department.

In 1998 he served four months in Vicenza, Italy at the Combined Air Operations Center supporting Operation Deliberate Guard in Bosnia-Herzegovina. While at the CAOC, he learned many facets of international weather forecasting operations. In July of 1998 he was assigned to the 10th Combat Weather Squadron to command a detachment supporting the 1st Special Forces Group (Airborne) at Fort Lewis, Washington on airborne status. While stationed at Fort Lewis, he routinely deployed overseas around the Pacific Region supporting the air and ground operations of the Special Operations Forces.

He entered the Meteorology Graduate program at the Air Force Institute of Technology in August 2000. Upon graduation, he will be assigned to the Air Force Weather Agency at Offutt AFB, Nebraska.

REPORT DOCUMENTATION PAGE

Form Approved
OMB No. 0704-0188

The public reporting burden for this collection of information is estimated to average 1 hour per response, including the time for reviewing instructions, searching existing data sources, gathering and maintaining the data needed, and completing and reviewing the collection of information. Send comments regarding this burden estimate or any other aspect of this collection of information, including suggestions for reducing the burden, to Department of Defense, Washington Headquarters Services, Directorate for Information Operations and Reports (0704-0188), 1215 Jefferson Davis Highway, Suite 1204, Arlington, VA 22202-4302. Respondents should be aware that notwithstanding any other provision of law, no person shall be subject to any penalty for failing to comply with a collection of information if it does not display a currently valid OMB control number.
PLEASE DO NOT RETURN YOUR FORM TO THE ABOVE ADDRESS.

1. REPORT DATE *(DD-MM-YYYY)*	2. REPORT TYPE	3. DATES COVERED *(From - To)*
26-03-2002	Master's Thesis	Jun 2001 - Mar 2002

4. TITLE AND SUBTITLE
VERIFICATION AND COMPARISON OF POLAR MM5 AND AFWA MM5 FORECASTS OVER ALASKA

5a. CONTRACT NUMBER

5b. GRANT NUMBER

5c. PROGRAM ELEMENT NUMBER

6. AUTHOR(S)
Courtemanche, William E., Captain, USAF

5d. PROJECT NUMBER

5e. TASK NUMBER

5f. WORK UNIT NUMBER

7. PERFORMING ORGANIZATION NAME(S) AND ADDRESS(ES)
Air Force Institute of Technology
Graduate School of Engineering and Technology (AFIT/EN)
2950 P. Street, Building 640
WPAFB, OH 45433-7765

8. PERFORMING ORGANIZATION REPORT NUMBER
AFIT/GM/ENP/02M-02

9. SPONSORING/MONITORING AGENCY NAME(S) AND ADDRESS(ES)
AFWA/DNXM
ATTN: Dr. Jerry Wegiel
106 Peacekeeper Dr.
Offutt AFB, NE 68113-4039 DSN: 271-3893

10. SPONSOR/MONITOR'S ACRONYM(S)

11. SPONSOR/MONITOR'S REPORT NUMBER(S)

12. DISTRIBUTION/AVAILABILITY STATEMENT
APPROVED FOR PUBLIC RELEASE: DISTRIBUTION UNLIMITED

13. SUPPLEMENTARY NOTES

14. ABSTRACT

The Mesoscale Model 5th Generation (MM5) is used for operational support to Air Force missions in the Alaskan Theater. The 11th Operational Weather squadron has identified problems with the MM5 producing excessively warm surface temperaturs. The Polar MM5 (PMM5), developed by the Byrd Polar Research Center for high latitude ice sheets, is tested over the Alaskan domains used by the Air Force Weather Agency to determine the utility in replacing the MM5 with the PMM5. The verification of surface temperature, pressure and wind as well as upper-air temperature, geopotential height, and relative humidity of 27-hour PMM5 forecasts are compared to the MM5 forecasts to assess the differences between the models' accuracies. A grid-to-station technique is used to compare model output to surface observation for 68 locations and to radiosonde upper-air observations for 7 locations.

The MM5 outperformed the PMM5 in root mean square error of all surface and upper-air parameters, while the PMM5 exhibited smaller biases in all fields. The differences between the models fell within the measurement accuracies of all parameters expect temperature. The analysis of horizontal features and comparison of domain biases alludes to a more physically realistic solution of the PMM5. The bottom line of site forecast accuracy precludes replacing the MM5 with the PMM5 at this time.

15. SUBJECT TERMS
Mesoscale Model, Polar Mesoscale Modelling, MM5, PMM5, Air Force Weather Agency, AFWA MM5, Numerical Weather Prediction, Model Comparison, Alaska Mesoscale Model, Alaska Temperature Forecast, Alaska Radiation, High-Latitude Radiation, High-Latitude Moisture, Atmospheric Temperature, Weather

16. SECURITY CLASSIFICATION OF:			17. LIMITATION OF ABSTRACT	18. NUMBER OF PAGES	19a. NAME OF RESPONSIBLE PERSON
a. REPORT	b. ABSTRACT	c. THIS PAGE			Lt Col Michael K. Walters, Ph.D., ENP
U	U	U	UU	94	19b. TELEPHONE NUMBER *(Include area code)* (937) 255-3636, ext 4681